https://doi.org/10.5194/egusphere-2026-4747
Preprint. Discussion started: 1 September 2026


# Decadal-scale monsoon seasonality and carbon burial response to the 4.2 ka event in the southwestern Bay of Bengal

**Mohd Salman[1, 2]*, Rajeev Saraswat[1]***

[1]Micropaleontology Laboratory, Geological Oceanography Division, National Institute of Oceanography, Goa, India

[2]School of Earth, Ocean and Atmospheric Sciences, Goa University, Goa, India

*For correspondence: salmanmicrop19@gmail.com, rsaraswat.nio@csir.res.in

## Abstract

The monsoon system is the primary driver of agricultural production, ecosystems, and societal development across the Indian subcontinent. However, monsoon's seasonal response to Holocene climate perturbations remains poorly constrained. The boundary between Northgrippian and Meghalayan ages, defined as the 4.2 ka event, is widely associated with Indian Summer Monsoon (ISM) failure, regional aridification, and the collapse of many civilizations. However, its precise timing, structure, and impact on monsoon seasonality, marine productivity, and carbon burial remains inadequately documented owing to the lack of decadal resolution marine records. Here, for the first time, we present a decadal resolution multiproxy marine record from the southwestern Bay of Bengal, integrating geochemical and planktic foraminiferal proxies to reconstruct the oceanographic response to the 4.2 ka event. We report a two-step decrease in carbon burial, beginning at 4.65 ± 0.17 ka and persisting until 3.97 ± 0.18 ka, spanning ~680 years. The event evolved through two phases, with Phase 1 (4.65-4.45 ka) characterized by a stronger but gradually weakened ISM, a moderate strengthening of the Indian Winter Monsoon (IWM), and enhanced terrestrial organic matter input, followed by Phase 2 (4.45-3.97 ka) marked by a pronounced and sustained ISM weakening and intensified IWM. We propose that the Atlantic Meridional Overturning Circulation triggered the 4.2 ka event, with a complex interaction of Inter Tropical Convergence Zone migration, El Niño-Southern Oscillation variability, and insolation changes operating across different timescales. Our findings establish a mechanistic link between altered monsoon seasonality and reduced carbon burial during the 4.2 ka event, highlighting how a climatically sensitive ocean basin can respond to short-term climatic perturbations.

**Keywords:** 4.2 ka event, teleconnections, monsoon seasonality, Productivity, Carbon burial, Planktic foraminifera, Bay of Bengal

https://doi.org/10.5194/egusphere-2026-4747
Preprint. Discussion started: 1 September 2026


## 1. Introduction

The Indian monsoon has a dominant control on agricultural production across the subcontinent, sustaining the livelihoods of over a billion people who depend on seasonal rainfall for irrigation and food security (Gagdil and Gagdil, 2006). Even a minor deviation from mean monsoon precipitation has cascading impact on food grain production, water availability, and regional economy, underscoring the societal necessity for accurate monsoon prediction (Prasanna, 2014; Gagdil and Gagdil, 2006; Kumar et al., 2004). Therefore, huge efforts are made to predict monsoons. Although several factors are found to affect monsoon, a complete understanding of the monsoon dynamics is still lacking, resulting in uncertain monsoon predictions. Understanding the monsoon intensity and its seasonal behavior under contrasting boundary conditions during the Holocene can help better comprehend monsoon dynamics (Banerji et al., 2020).

Initially, the Holocene was believed to be climatologically stable. However, the high-resolution records revealed the prevalence of extreme climatic events during the Holocene (Wang et al., 2005; Fleitmann et al., 2003; Gupta et al., 2003). A prominent climatic anomaly that occurred at the boundary between the Northgrippian and Meghalayan ages of the Holocene Epoch is defined as the 4.2 ka event (Walker et al., 2019). The 4.2 ka event has been reported as a cold and dry event in the mid to low-latitude regions of the Northern Hemisphere (Giesche et al., 2023; Banerji et al., 2020; Ran and Chen, 2019). The climatic anomaly at 4.2 ka left profound imprints not only on natural climatic systems but also on the human societies, leading to the collapse of many civilizations including the Egyptian Old Kingdom in the Nile Valley, the Akkadian Empire in Mesopotamia, and the Harappan civilization of the Indus Valley (Railsback et al., 2018; Stanley et al., 2003, Staubwasser et al., 2003; Cullen et al., 2000). Despite of the growing interest in 4.2 ka event, the driving mechanisms including the effect of solar forcing, El-Nino Southern Oscillation (ENSO), Indian Ocean Dipole (IOD), and shift in Inter-Tropical Convergence Zone (ITCZ) in modulating this event, remains poorly constrained (Banerji et al., 2020; Toth and Aroson, 2019). In particular, teleconnections of the North Indian Ocean with the Atlantic Meridional Overturning Circulation (AMOC) and ENSO-IOD during this interval are insufficiently understood due to the lack of high-resolution palaeoclimatic records capable of resolving decadal to multidecadal variability. The 4.2 ka event doesn't exhibit a strong evidence of meltwater flux from the high-latitude ice sheets unlike the 8.2 ka event (Gerber et al., 2025; Mayeski et al., 2004). Although, a majority of the studies suggest it as a climatic event, its beginning and end are not properly defined (Sharifi et al., 2015;

https://doi.org/10.5194/egusphere-2026-4747
Preprint. Discussion started: 1 September 2026


Berkelhammer et al., 2012; Cullen et al., 2000). Additionally, the transition differs regionally in its climatological and chronological signatures (Helama, 2024).

Indian monsoon, a vital component of the world's climate system, also experienced a disruption during the 4.2 ka event (Sengupta et al., 2020; Saraswat et al., 2016; Prasad et al., 2014; Dixit et al., 2014; Staubwasser et al., 2003; Kudrass et al., 2001). However, the implications of this event are mixed, with some areas experiencing droughts and others receiving extensive rainfall (Booth et al., 2005; Staubwasser et al., 2003; Cullen et al., 2000). The erratic weather patterns associated with the event likely harmed agriculture and water resource management. The mismatch in climatic implications of 4.2 ka event is because of the difference in the monsoon seasonality in different parts of the Indian subcontinent. Therefore, further research is needed to constrain the winter expression of the 4.2 ka event and to disentangle the seasonal monsoon signals across the Asian monsoon regions. The Indian subcontinent is at the heart of the Asian monsoon system where it receives a huge summer as well as winter monsoon precipitation (Dai et al., 2023). The majority of the rivers from the Indian subcontinent drain into the Bay of Bengal. The southwestern Bay of Bengal (swBoB) receives an enormous amount of riverine influx during both the summer and winter monsoon seasons (Sandeep and Pant, 2019; Vinayachandran et al., 2013). Therefore, the swBoB can be a potential site to reconstruct the monsoon seasonality during the extreme climatic events of the Holocene.

Several workers have reconstructed the summer monsoon intensity in the past, from the western Bay of Bengal (Suokhrie and Saraswat, 2024; Suokhrie et al., 2021; Gautam et al., 2021; Ankit et al., 2017; Da Silva et al., 2017; Phillips et al., 2014; Ponton et al., 2012; Rashid et al., 2011; Govil and Naidu, 2011; Kudrass et al., 2001). Many lake sediment, speleothem and pollen records have also been used to reconstruct the summer monsoon intensity during the Holocene from the Indian subcontinent (Dixit et al., 2018; Dutt et al., 2018; Prasad et al., 2014; Berkelhammer et al., 2012). However, the records of winter monsoon intensity during the past, especially during the 4.2 ka event, are limited (Verma et al., 2022). Additionally, most of the marine records from the Bay of Bengal don't have the temporal resolution to precisely define sub-centennial monsoon intensity changes during the Holocene (Verma et al., 2022; Liu et al., 2021; Gautam et al., 2021; Paketi et al., 2021; Ankit et al., 2017; Da Silva et al., 2017; Sijinkumar et al., 2016; Phillips et al., 2014; Ponton et al., 2012; Rashid et al., 2011; Govil and Naidu, 2011; Kudrass et al., 2001). Therefore, high-resolution marine records are required to

https://doi.org/10.5194/egusphere-2026-4747
Preprint. Discussion started: 1 September 2026


understand the monsoon seasonality, productivity and carbon burial response to major and short-term climatic events during the Holocene.

Planktic foraminifera, owing to their high sensitivity to even subtle environmental fluctuations, serve as a reliable proxy for paleoclimate reconstruction (Salman and Saraswat, 2024; Saraswat, 2015, Katz et al., 2010; Nigam, 2005). Their fossilized remains provide insights into past oceanographic conditions through species abundance and geochemical signatures preserved in their calcite shells (Schiebel and Hemleben, 2017). The abundance of total planktic foraminifera, species abundance, and their assemblages are frequently used for precise reconstruction of the past oceanographic conditions and climate dynamics (Kucera, 2007). By integrating faunal assemblages and bulk sediment geochemistry data, planktic foraminifera proxies offer a robust framework to understand long-term ocean-climate interactions.

Marine sediments are reliable archives of long-term carbon burial, integrating both organic and inorganic carbon fluxes. The accumulation of carbon in marine sediments is influenced by primary productivity, terrestrial input, and preservation conditions at the seafloor (Hedges and Keil, 1995; Cartapanis et al., 2016). The ocean plays a central role in the global carbon cycle, and the changes in marine carbon burial at different climatic boundaries have significant implications for atmospheric $CO_2$ concentrations and long-term climate feedbacks (Francois et al., 1997). However, the response of marine carbon burial to short-term climatic perturbations such as the 4.2 ka event remains poorly documented. The shifts in summer and winter monsoon intensity simultaneously alter riverine discharge, surface ocean productivity, water column stratification, and organic matter preservation, all of which directly modulate the quantity and source of carbon reaching the seafloor (Saraswat et al., 2023a; Suokhrie et al., 2021; Kessarkar and Rao, 2007). Quantifying these changes at decadal resolution is therefore essential not only to understand the oceanographic response to the 4.2 ka event but also to assess how short-term climatic perturbations influence the marine carbon cycle in a climatically sensitive ocean basin.

We present a decadal resolution multi-proxy marine sediment record of monsoon seasonality, productivity, and long-term carbon burial changes during the 4.2 ka event from the swBoB, a region strongly influenced by Indian summer and winter monsoons. We have used the planktic foraminifera assemblages to differentiate between the summer and winter monsoon seasonality.

https://doi.org/10.5194/egusphere-2026-4747
Preprint. Discussion started: 1 September 2026


## 2. Geological and Oceanographic Setting

The Cauvery basin is one of the major peri-cratonic rift basins that developed during the rifting processes associated with the breakup of the Gondwana supercontinent during the Mesozoic Era. As the Indian Plate separated from Madagascar, rift valleys formed, leading to the development of the Cauvery basin (Twinkle et al., 2016). The Cauvery River deposits a huge amount of sediment resulting in a very high sedimentation rate in the basin. The river discharge and sediment load in the Cauvery River peaks during the month of November (Vaithiyanathan et al., 1988). The topography and gradient of the land around the Cauvery River basin play a crucial role in the high sedimentation rate. The river originates from the Western Ghats, with steep slopes, leading to more physical weathering. As the river flows toward the coast, it cuts through various types of terrain, including rocks, soils, and sediments, carrying more sediment along the way (Vybhav et al., 2020; Vaithiyanathan et al., 1988; Subramanian, 1978). The Cauvery River also forms a delta, near the river mouth, where the sediments are deposited. The delta acts as a natural sediment trap, slowing down the flow and allowing the sediments to settle on the seafloor. This process contributes to offshore sediment accumulation (Alappat et al., 2010; Singh and Rajamani, 2001). Out of the entire shelf of the western Bay of Bengal, the highest sand content was reported near the Cauvery River (Jacob et al., 2008).

The land and ocean thermal contrast results in moisture-laden winds blowing over Indian subcontinent from June to August (**Fig. 1**). The intertropical convergence zone reaches its northernmost position by August resulting in ~70% rainfall over India (Dixit and Tandon, 2016). Later, as the ITCZ recedes southward, reaching its southernmost position in January, a reversal in pressure gradient triggers the onset of the winter monsoon, mainly over southeast India. From the wind rose diagram, it is evident that the high frequency of winds in the Cauvery basin is from the northeast during the winter season (**Fig. 1c**). Because of these intense northeast winds, Tamil Nadu receives intense precipitation during the winter season (October to December) (Kripalani and Kumar, 2004; Khole and De, 2003) (**Fig. 1b**). Thus, the winter monsoon is the predominant rainy season in Tamil Nadu accounting for approximately ~60% of the rainfall in the coastal areas and nearly 40−50% in the interior districts (Khole and De, 2003). The Krishna, Pennar, and Cauvery rivers discharge substantial amounts of freshwater into the swBoB during both the summer and winter monsoon seasons (Khole and De, 2003; Krishnamurthy and Shukla, 2000). However, the freshwater discharge of Cauvery River dominates from October to December (**Fig. 1b**). In the swBoB, the seasonal variation in sea surface salinity is around 1 psu (**Fig. 2**), with a minimum during early winter (November –

https://doi.org/10.5194/egusphere-2026-4747
Preprint. Discussion started: 1 September 2026


December). This decrease in salinity is attributed to the precipitation associated with the winter monsoon over southeast India (Dimri et al., 2016).

The North Indian Ocean experiences a semi–annually reversing monsoon wind pattern (Vinayachandran et al., 2002; Schott and McCreary, 2001). The seasonal winds induce a reversal of circulation along the east and west coasts of India (Shankar et al., 2002). At the onset of the summer season, the summer monsoon current (SMC) transports high salinity water from the southeastern Arabian Sea (seAS) into the swBoB (**Fig. 1**). It joins the East India Coastal Current (EICC) and flows towards the north (**Fig. 1**). From June to September, SMC transports approximately 10 Sv (Sverdrups) of water into the Bay of Bengal (Vinayachandran et al., 1999). Simultaneously, there is an influx of high salinity and carbonate–enriched water from the Gulf of Mannar to the Palk Bay, estimated at ~16.301 $m^3/s$. This high salinity carbonate-enriched water subsequently flows into the swBoB and enhances carbon burial in this region (Salman and Saraswat, 2024; Jagadeesan et al., 2013).

The Bay of Bengal exhibits relatively lower primary productivity as compared to the Arabian Sea. The diminished productivity in the Bay of Bengal is primarily attributed to the extensive cloud cover, sediment load, stratification, and a narrow shelf (Sarma et al., 2016; Prasanna Kumar et al., 2010; 2004; 2002; Madhupratap et al., 2003; Gomes et al., 2000). The Bay of Bengal also experiences weak coastal upwelling and winter convective mixing as compared to the Arabian Sea (Prasanna Kumar et al., 2002; Shetye et al., 1991). However, the eddies and gyres are common in the Bay of Bengal and enhance the productivity in the area (Jayalakshmi et al., 2015; Sabu et al., 2015; Prasanna Kumar et al., 2010; 2004; 2002; Muraleedharan et al., 2007; Vinayachandran et al., 2005). During the winter season, cyclonic eddies that bring nutrient-rich and cold water to the surface are common in the swBoB resulting in a cooler sea surface temperature, while in the summer season, the anticyclonic eddies are more prevalent leading to a warmer sea surface temperature (Jayalakshmi et al., 2015; Chen et al., 2013).

The southwestern Bay of Bengal experiences warmer sea surface temperature (SST) during the summer season ranging from 28.5 to 29.5 °C (**Fig. 2**). The sea surface salinity (SSS) is however low during this season ranging from 32.5 to 34 psu. A relatively cooler SST is observed during the winter season ranging from 26 to 27.5°C and SSS is also low in the swBoB ranging from 32 to 33.5 psu. The Chlorophyll-a is relatively high in marginal areas in the swBoB during the summer season (**Fig. 2**). However, the Chlorophyll-a content remains low during the winter season suggesting relatively higher marine productivity during the summer season (**Fig. 2**).

https://doi.org/10.5194/egusphere-2026-4747
Preprint. Discussion started: 1 September 2026


## 3. Materials and Methods

The sediments from a piston core (SSD067 PC03) recovered during the 67th cruise of RV *Sindhu Sadhana* (SSD067), from the swBoB, off Cauvery River mouth (Latitude 11.4202°N, Longitude 80.0323°E) at a water depth of 509 m were used for this work (**Fig. 1**). The piston core was 15.72 m long and mainly comprised of homogeneous, olive-grey hemipelagic mud (silt+clay), with no visible turbidite deposits or sedimentary disturbances. A section of this core (101 cm between 3.59 m and 4.60 m) was used for this study. The absence of coarse-grained intercalations and the uniformly fine-grained nature of the sediments in the studied section was consistent with continuous pelagic sedimentation at the core site, located at the upper continental slope off the Cauvery River mouth.

The sediment core was sub-sampled at an interval of 1 cm and the samples were processed by following the standard procedure (Salman and Saraswat, 2024). Approximately 10-15 g of wet sediments were freeze-dried. About 1-2 g of the dried sediments were separated for geochemical analysis and the rest was wet sieved with 63 µm sieve to separate the foraminiferal shells. A total of 101 powdered sediment samples, at an interval of 1 cm, were used for the geochemical analysis. One-fourth of >63 µm fraction was dry sieved with 150 µm mesh to pick the planktic foraminifera. A representative aliquot of the sieved coarse fraction obtained after coning and quartering was weighed and spread in a picking tray to pick planktic foraminifera. A minimum of 300 specimens of planktic foraminifera were picked from the alternate intervals. The picked foraminiferal shells were identified upto the species level by following the published literature (Schiebel and Hemleben, 2017; Shrivastav et al., 2016; Ovechkina et al., 2010; Hemleben et al., 1989; Parker, 1962). The abundance of planktic foraminifera was calculated as the number per gram of dry sediment (TPN).

The seasonal preferences of planktic foraminiferal species were considered based on their modern distribution patterns documented in surface sediments (core-top), plankton tow, and sediment trap studies. Species-specific seasonal preferences in the swBoB and western Bay of Bengal are well established. *Globigerinoides ruber*, *Globigerina bulloides*, *Neogloboquadrina dutertrei*, *Trilobatus trilobus*, *Trilobatus sacculifer*, *Globigerinella siphonifera*, and *Neogloboquadrina incompta* attain peak relative abundances during the summer monsoon season and were collectively used here as the summer monsoon assemblage (Salman and Saraswat, 2024; Maeda et al., 2022; Bhadra and Saraswat, 2021; Stoll et al., 2007; Guptha et al., 1997). In contrast, *Globigerinita glutinata*, *Globigerina falconensis*, *Globorotalia menardii*, and *Pulleniatina obliquiloculata* reach their highest relative

https://doi.org/10.5194/egusphere-2026-4747
Preprint. Discussion started: 1 September 2026


abundances under winter monsoon conditions and constitute the winter monsoon assemblage (Salman and Saraswat, 2024; Maeda et al., 2022; Bhadra and Saraswat, 2021; Stoll et al., 2007; Guptha et al., 1997). Among individual species, *G. ruber* thrives under warm, oligotrophic, and well-stratified surface ocean conditions, whereas *G. bulloides* is associated with cooler, nutrient-enriched waters driven by upwelling and vertical mixing (Salman and Saraswat, 2024; Bhadra and Saraswat, 2021; Stoll et al., 2007). The contrasting ecological preferences of these two species make the *G. bulloides*/*G. ruber* ratio a useful proxy for reconstructing past changes in sea surface temperature, marine productivity, upwelling intensity, and stratification.

The seasonal sea surface temperature and salinity were obtained from the World Ocean Atlas 2018 and Chlorophyll-a was accessed through the Live Access Server of CSIR-National Institute of Oceanography, Goa, India (Locarnini et al., 2019; Zweng et al., 2019). The hourly wind speed and direction data at a height of 10 m for the year 2021 were obtained from the NASA POWER Data Access Viewer (https://power.larc.nasa.gov/data-access-viewer/) and utilized to generate a wind rose diagram using WRPLOT view software. The monthly mean rainfall data for Tamil Nadu was sourced from the Centre for Hydrometeorology and Remote Sensing (CHRS) RainSphere platform (https://rainsphere.eng.uci.edu/), while freshwater discharge data for the Cauvery River was acquired through the Group on Earth Observations (GEO) HydroViewer, a platform dedicated to global water sustainability (https://hydroviewer.geoglows.org).

### 3.1 Carbon and Nitrogen Analysis

The freeze-dried sediments were powdered with the help of agate mortar and pestle for geochemical analysis. The Flash 2000 series CN Elemental Analyzer was used to analyze the total carbon (TC) and nitrogen (N) content of the sediment. The NC soil was used as the calibration standard for TC and N with the values of 2.29 ± 0.07% and 0.21 ± 0.01%, respectively. The standard deviation and associated error for TC were ± 0.05% and 2.24% and for N ± 0.01% and 4.61%, respectively. The total inorganic carbon (TIC) was analyzed by using a $CO_2$ Coulometer (CM5017O UIC). The analytical-grade calcium carbonate ($CaCO_3$) standard, with inorganic carbon of 12%, was used for TIC analysis. The standard deviation was ± 0.070 % and the associated error was 0.58%. The organic carbon ($C_{org}$) was obtained by subtracting the inorganic carbon from the total carbon. The $CaCO_3$ percentage in the bulk sediment was calculated from TIC and the atomic weight of carbon in $CaCO_3$.

https://doi.org/10.5194/egusphere-2026-4747
Preprint. Discussion started: 1 September 2026


### 3.2 Chronology

The radiocarbon ($^{14}C$) dating is commonly used to estimate the age of carbon-bearing materials (e.g. foraminifera, corals, stalagmites, trees, sediments) deposited in natural environment during the last ~55 kyr. We used planktic foraminifera to develop the chronology of the piston core. The dried coarse fraction (>63 µm) was sieved with 125 µm mesh to pick the planktic foraminifera. Due to the less availability of the carbonate, the mixed planktic foraminifera were picked for the $^{14}C$ analysis. The chronology of the core was established using 36 accelerator mass spectrometer (AMS) radiocarbon dates analyzed at the Inter-University Accelerator Center, New Delhi, India. For the studied section, the seven dates were spaced at an interval of around 25 cm, ranging from 350-500 cm (**Fig. 3, Table 1**). All the $^{14}C$ ages were calibrated by using Marine20 calibration curve in the CALIB 8.2 radiocarbon calibration program (Heaton et al., 2020) with a reservoir correction (ΔR) and uncertainty of -106 ± 20 years for the swBoB (Dutta et al., 2001a; 2001b; 2001c).

### 3.3 Z-score Calculations

For the regional comparison of multiproxy records, Z-score standardization was applied to each proxy individually using the following transformation:

$$\mathbf{Z = (x - \mu) / \sigma}$$

Where x is the observed value, μ is the record mean, and σ is the standard deviation. This eliminated differences arising from different proxy types and the varying range of values across the records. It converts all data to dimensionless units where individual values reflect their relative deviation from the mean value of the studied section, thus facilitating direct inter-comparison across records.

## 4. Results

### 4.1 Temporal resolution and chronological control

The studied section spans 3.82 to 5.16 ka, with an average sedimentation rate of 80.28 cm/kyr corresponding to ~12 years of deposition time/cm, providing near-decadal scale temporal resolution (**Fig. 3**). Three of the seven radiocarbon dates fall within the event interval itself (4.69 ± 0.17 ka, 4.31 ± 0.18 ka, and 3.96 ± 0.18 ka), directly falling at the onset, middle, and termination of the prolonged 4.2 ka event rather than relying solely on interpolation between distant date points (**Fig. 3**). This robust chronological control substantially reduces age uncertainty across the event interval and lends confidence to the reported timing from 4.65 to

https://doi.org/10.5194/egusphere-2026-4747
Preprint. Discussion started: 1 September 2026


3.97 ka and duration of 680 years. The 2σ age uncertainties at the event onset (4.65 ka) and termination (3.97 ka) are ± 165 and ± 175 years, respectively, confirming that the claimed event boundaries are resolved at around a centennial scale, which is smaller than the event duration of 680 years.

## 4.2 Geochemical characteristics

A prominent shift in all geochemical proxies was observed between 4.65 and 3.97 ka during the Northgrippian-Meghalayan transition, coinciding with 4.2 ka event. A two-step decrease in CF, TC, TIC and N was evident during phase 1 and phase 2, whereas $C_{org}$ and $C_{org}$/N ratio increased during phase 1 and subsequently decreased during phase 2 (**Fig. 4; Table 2**). The mean values of CF, TC, TIC and N decreased from 2.41%, 3.67%, 1.33% and 0.24%, respectively, during the pre-event interval to 1.97%, 3.41%, 0.92% and 0.22% during phase 1, followed by a further decrease to 1.49%, 2.88%, 0.81% and 0.20% during phase 2 (**Table 2**). Although, a minor increase was observed during the post event interval, the values remained lower than those during the pre-event interval (**Fig. 4; Table 2**). Similarly, $CaCO_3$ content decreased abruptly at 4.65 ka and remained low until 3.97 ka (**Fig. 7**). The pre-event mean value of $C_{org}$ and $C_{org}$/N were 2.35% and 9.96, respectively, and increased to 2.49% and 11.43 during phase 1 of the event. However, the $C_{org}$ mean value decreased sharply to 2.07% during phase 2 (**Table 2**). A similar trend was observed in $C_{org}$/N ratio, which increased abruptly at 4.65 ka, followed by a gradual decrease until 3.97 ka (**Fig. 7**). Throughout the studied interval, $C_{org}$/N ranged between 9.5 and 12. The correlation analyses revealed a significant positive relationship between CF and TPN ($R^2$ = 0.67, p < 0.001, n = 51), CF and $CaCO_3$ ($R^2$ = 0.64, p < 0.001, n = 101), $CaCO_3$ and TPN ($R^2$ = 0.40, p < 0.001, n = 51) (**Fig. 5**). Additionally, $CaCO_3$ also had a significant positive but relatively weak correlation with $C_{org}$ ($R^2$ = 0.28, p < 0.001, n = 101). However, it showed a separate cluster because $CaCO_3$ and $C_{org}$ behaved oppositely during phase 1 of the event (**Fig. 5d**). Except between $CaCO_3$ and $C_{org}$ during phase 1 of the 4.2 ka event, these relationships indicate a statistically significant covariation among the measured geochemical and planktic foraminiferal proxies throughout the studied section.

## 4.3 Relative abundance of planktic foraminifera species and their assemblages

All the planktic foraminifera in the studied section belonged to 27 species. Among the 27 planktic foraminifera species, six were considered as dominant (having an average relative abundance >5%) (**Fig. 6**). *Globigerina bulloides* was the most abundant species throughout the

https://doi.org/10.5194/egusphere-2026-4747
Preprint. Discussion started: 1 September 2026


record. The mean relative abundance of *G. bulloides* during the pre-event interval closely resembled those observed during phase 1 of the prolonged 4.2 ka event (**Table 2**). However, a decrease in its mean relative abundance was recorded during phase 2, whereas it was relatively higher during phase 1. Comparatively, a more prominent shift was observed in relative abundance of *G. ruber* during phase 2 of the 4.2 ka event (**Fig. 6**). Its mean relative abundance was 16.46% during phase 1 but decreased sharply to 10.85% during phase 2. Subsequently, it increased to 13.44% during the post-event interval (**Table 2**). The relative abundance of *N. dutertrei*, a thermocline dwelling species, decreased abruptly at 4.65 ka and remained relatively low throughout the event (**Fig. 6; Table 2**). In contrast, the mean relative abundance of *G. glutinata* remained relatively stable across the pre-, phase 1, and post-event intervals. A prominent increase in its abundance was observed around the canonical 4.2 ka event (**Fig. 6**). The abundance of *T. sacculifer* was comparatively lower during the event and increased during the post-event interval. A prominent increase in the abundance of *P. obliquiloculata* was observed during the prolonged 4.2 ka event. The highest abundance of planktic foraminifera was at 4.7 ka, after which it gradually decreased until 3.8 ka (**Fig. 6**). The mean relative abundance of SMA during the pre-event interval and phase 1, were nearly identical. However, SMA showed a gradual declining trend throughout phase 1 and decreased abruptly during phase 2 of the event **(Fig. 7**; **Table 2**). Conversely, a distinct increase in the relative abundance of WMA was observed during the 4.2 ka event, with the highest mean WMA abundance being during phase 2 (**Fig. 7**; **Table 2**). The simultaneous decrease in SMA and increase in WMA indicates a weakening of the summer monsoon and strengthening of winter monsoon during the event. Furthermore, the *G. bulloides*/*G. ruber* ratio increased substantially during phase 2, suggesting a significant shift in upper-ocean hydrographic conditions associated with 4.2 ka event (**Fig. 7**).

## 5. Discussion

### 5.1 Onset, duration, and carbon burial response to the 4.2 ka event

The sediment geochemistry and foraminiferal data indicate that the prolonged 4.2 ka event began at 4.65 ± 0.17 ka and terminated at 3.97 ± 0.18 ka, with a total duration of 680 years (**Fig. 4, 6, 7**). The onset of the event is not uniform in all the records therefore the duration of the event also varies between different records (Giesche et al., 2019; Railsback et al., 2018; Dixit et al., 2014; Berkelhammer et al., 2012; Cullen et al., 2000). In some records, the event lasted for one or two centuries, while in others, the changes were observed for a longer duration. The duration reported in this study is among the longest reported for the 4.2 ka event so far and

https://doi.org/10.5194/egusphere-2026-4747
Preprint. Discussion started: 1 September 2026


is consistent with some previous observations (Saraswat et al., 2023a; Saravanan et al., 2019; Railsback et al., 2018; Dixit et al., 2018). The chronology is particularly robust because three radiocarbon dates (4.69 ± 0.17 ka, 4.31 ± 0.18 ka, and 3.96 ± 0.18 ka) directly constrain the event interval, reducing reliance on interpolation and providing high confidence in the timing of the onset and termination. The earliest beginning of the event was reported from the Thar desert at 4.7 ka (Enzel et al., 1999), whereas the late termination was reported at 3.41 ka (Psomiadis et al., 2018), highlighting the spatially heterogeneous expression of this climatic event. The high temporal resolution of the present record, therefore, provides an opportunity to study the detailed evolution of the event in the North Indian Ocean.

A notable feature of the event is that the carbon burial response evolved through two distinct phases rather than a single prolonged interval of environmental deterioration. The first phase (4.65 - 4.45 ka) was characterized by a decrease in CF, TC, $CaCO_3$, and N, indicating an initial reduction in marine productivity (**Fig. 4, 7**). In contrast, $C_{org}$ and $C_{org}$/N ratio increased during this interval. The second phase (4.45-3.97 ka) was characterized by a further reduction in all geochemical proxies, including $C_{org}$, along with low planktic foraminiferal abundance, indicating a further suppression of marine productivity and carbon burial (**Fig. 4, 6, 7**). These contrasting trends suggest that different mechanisms controlled the carbon burial during the two phases of the event. The $C_{org}$/N ratio is widely used to distinguish the source of sedimentary organic matter (Suokhrie et al., 2021; Saalim et al., 2021; Kessarkar and Rao, 2007; Lamb et al., 2006). Marine phytoplankton typically exhibit $C_{org}$/N ratio between 4 and 10, reflecting their protein-rich composition and proximity to the Redfield ratio (C/N = 6.6). In contrast, terrestrial vascular plants generally has $C_{org}$/N ratios >20 due to their high cellulose and lignin contents (Meyers, 1994). The sediments with $C_{org}$/N ratio between 10 and 20 are interpreted as containing a mixture of marine and terrestrial organic matter sources (Lamb et al., 2006; Meyers, 1994). Throughout the studied interval, the $C_{org}$/N values ranged from 9 to 12, indicating a mixture of marine and terrestrial organic matter sources. The increase in $C_{org}$/N ratio at 4.65 ka suggests an increased terrestrial influence on the sedimentary organic matter pool. Because marine productivity proxies were already decreasing, the higher $C_{org}$/N values likely resulted from a combination of enhanced terrestrial organic matter contribution and reduced production of N-rich marine organic matter. The $C_{org}$/N ratio during phase 2 further supports this mechanism. If the higher $C_{org}$/N values were solely a result of reduced marine productivity, the ratio was expected to increase further during phase 2. Instead, $C_{org}$/N decreased during phase 2 despite continued reduction in productivity proxies such as CF, TPN, $CaCO_3$ and N. This pattern suggests that the increase in $C_{org}$/N during phase 1 reflects greater

https://doi.org/10.5194/egusphere-2026-4747
Preprint. Discussion started: 1 September 2026


relative influence of terrestrially derived organic matter, whereas phase 2 was characterized by reduced contributions from both marine and terrestrial carbon sources. Consequently, the two phases represent distinct modes of carbon burial response. However, the relatively higher $C_{org}$/N ratio during the prolonged 4.2 ka event compared to prior and post event intervals indicates diagenetic alteration or preferential degradation of a portion of N-rich marine organic matter. The increased terrestrial input and the influence of oxygenated water due to stronger winter monsoon would lead to a poor preservation of organic matter. The poorly preserved organic matter has low N content and thus a higher $C_{org}$/N ratio (Suokhrie et al., 2021; Saalim et al., 2021; Kessarkar and Rao, 2007).

The coarse fraction (CF) includes both the biogenic shells and sandy lithogenic sediments flux (Salman and Saraswat, 2024; Saraswat et al., 2023a). Interestingly, we did not find any lithogenic sediment in >63 μm fraction. The coarse fraction contained only biogenic shells throughout the studied interval. Therefore, the lithogenic sediments were completely muddy (silt + clay). The significant positive correlation of CF with TPN and $CaCO_3$ (**Fig. 5**) confirms that it was mainly controlled by biogenic shell flux. However, the positive correlation between TPN and $CaCO_3$ ($R^2$ = 0.40, $p < 0.001$, n = 51) indicates that the planktic foraminifera contributed only 40% of the total $CaCO_3$ content, and the rest was contributed by other calcareous organisms. Schiebel (2002) estimated that only planktic foraminifera can contribute from 32 to 80% of $CaCO_3$ to the global deep ocean calcite budget. Therefore, the changes in calcareous shell flux play a significant role in carbonate burial.

A positive but relatively weak correlation between $C_{org}$ and $CaCO_3$ ($R^2$ = 0.28, $p < 0.001$, n = 101) suggests that the organic and inorganic carbon burial was not only governed by productivity but also by additional factors such as changes in terrigenous sources and carbonate production, which influenced the total carbon burial during the prolonged 4.2 ka event. A separate cluster in correlation plot between $C_{org}$ and $CaCO_3$ (**Fig. 7d**) suggests that $C_{org}$ and $CaCO_3$ behaved oppositely due to increase in terrestrially derived organic matter during phase 1 of the 4.2 ka event as evident from the higher $C_{org}$/N ratio. The carbonate dissolution is unlikely to have affected the $CaCO_3$ because the core was recovered from a water depth of 509 m, well above the modern lysocline in the western Bay of Bengal (Salman and Saraswat, 2024; Bhadra and Saraswat, 2023). The decrease in carbonate burial can also be amplified by hydrographic changes affecting the calcification. The SMA and WMA suggest that the Indian Summer Monsoon (ISM) was relatively weaker while the Indian Winter Monsoon (IWM) was stronger during the prolonged 4.2 ka event (**Fig. 7**). As the ISM weakens, SMC slows down,

https://doi.org/10.5194/egusphere-2026-4747
Preprint. Discussion started: 1 September 2026


thus reducing the influx of high salinity Arabian Sea water to the study area (Dimri et al., 2016; Vinayachandran et al., 1999). The weaker ISM also means reduced influx of the Gulf of Mannar and Palk Bay's high salinity water into the swBoB. Additionally, the EICC during the winter season, which carries low salinity water from the north to the study site, was relatively stronger due to stronger IWM, creating a low salinity gradient in the swBoB. Therefore, the synchronous decrease in TPN and $CaCO_3$ may also be attributed to the low salinity during the prolonged 4.2 ka event. The calcareous organisms produce lighter shells in less saline water (Zarkogiannis et al., 2022; Trask, 1938), thereby resulting in low $CaCO_3$ flux. Therefore, the carbonate burial was controlled not only by productivity but also by changes in calcification intensity.

Our record suggests that the prolonged 4.2 ka event evolved through two successive stages. Phase 1 represents a transitional interval characterized by declining marine productivity but increased terrestrial influence on sedimentary organic matter, resulting in elevated $C_{org}$ and $C_{org}$/N values despite a reduction in carbonate-related proxies. Phase 2 represents a threshold response during which marine productivity decreased further and terrestrial carbon contribution also diminished, leading to a decrease in both organic and inorganic carbon burial. This two-phase model provides a new perspective on the evolution of the 4.2 ka event in the North Indian Ocean and highlights the complex interaction among monsoon seasonality, marine productivity, and carbon cycling during a Holocene climatic perturbation.

### 5.2 Planktic foraminiferal response to the 4.2 ka event

The dominant planktic foraminiferal species exhibited contrasting response to the prolonged 4.2 ka event, reflecting changes in seasonal monsoon forcing that affected surface-water hydrography, thermocline structure, and productivity. The differing timing and magnitude of species-specific response suggests that the event evolved progressively rather than as an abrupt climatic perturbation. *Globigerina bulloides* was the most abundant species throughout the studied interval. The mean abundance of *G. bulloides* remained broadly similar during the pre-event interval and phase 1 of the 4.2 ka event, although a decrease was observed during phase 2 (**Fig. 6; Table 2**). In low-latitude oceans, *G. bulloides* is associated with nutrient-rich waters and upwelling-induced high productivity (Schulz et al., 2002; Naidu et al., 1999; Reynolds and Thunell, 1985; Cullen and Prell, 1984). The relatively stable abundance of *G. bulloides* suggests that productivity did not collapse abruptly at the onset of the event. Instead, the gradual decline in its abundance during phase 2 is consistent with the progressive reduction in productivity inferred from decreasing TPN, CF, $CaCO_3$, $C_{org}$, and N. The relatively stable abundance of *G. bulloides* during phase 1 also suggests that the ISM was strong enough with

https://doi.org/10.5194/egusphere-2026-4747
Preprint. Discussion started: 1 September 2026


a gradual decrease in its intensity as observed by a gradual decrease in SMA. However, the decline in *G. bulloides* abundance during phase 2 suggests a significant decrease in ISM intensity.

*Globigerinoides ruber* exhibited one of the most pronounced response to the event. Its abundance remained relatively high during phase 1 but declined sharply during phase 2 before partially recovering in post event interval (**Fig. 6**). *Globigerinoides ruber* prefers well-stratified, warmer, and oligotrophic conditions (Salman and Saraswat, 2024; Saraswat et al., 2023b; Bhadra and Saraswat, 2021; Guptha et al., 1997). An abrupt decrease in *G. ruber* at 4.45 ka suggests cooler SST and weaker upper ocean stratification during the phase 2 of the 4.2 ka event. The sediment trap studies have suggested that the highest shell flux of *G. ruber* in the swBoB was associated with the summer season (Maeda et al., 2022; Guptha et al., 1997). Therefore, its low abundance indicates relatively cooler summers during phase 2 of the 4.2 ka event. However, the high abundance of *G. ruber* during phase 1 suggests that the summer season remained relatively warmer as compared to phase 2. The decline in *G. ruber* and *G. bulloides* at 4.45 ka also indicates that the major weakening of ISM occurred during phase 2 of the event even though it had been gradually declining during phase 1, which is also evident by SMA (**Fig. 6**).

Interestingly, the response of *N. dutertrei* was synchronous with carbon burial and its abundance decreased from the high of ~14% at 4.65 ka to the lowest of ~6% during the 4.2 ka event **(Fig. 6)**. *Neogloboquadrina dutertrei* is a thermocline-dwelling species commonly associated with warm and low salinity subsurface waters and subsurface chlorophyll maxima (Yadav et al., 2022; Schiebel and Hemleben, 2017; Guptha et al., 1997). The high abundance of *N. dutertrei* was also reported in subsurface low salinity regions from the northern and western BoB (Salman and Sarasawat, 2024, Bhadra and Saraswat, 2021). The synchronous timing of the decrease in its relative abundance with the onset of geochemical changes indicates the change in thermocline hydrography. The abrupt decrease in *N. dutertrei* abundance therefore suggests a reduction in subsurface productivity together with a drop in temperature and increase in salinity of the thermocline during the prolonged 4.2 ka event.

The mean abundance of *G. glutinata* remained relatively stable during the pre-event, event, and post-event intervals (**Fig. 6; Table 2**). *Globigerinita glutinata* is a cosmopolitan species characterized by broad ecological tolerance and widespread distribution across different oceanographic settings (Mazumder et al., 2009; Hemleben et al., 1989). Although it is abundant in subtropical and temperate waters (Schmuker and Schiebel, 2002; Schiebel and Hemleben, 2000), higher abundance has also been reported from tropical regions having high

https://doi.org/10.5194/egusphere-2026-4747
Preprint. Discussion started: 1 September 2026


nutrient availability (Mazumder et al., 2009; Schiebel et al., 2001). In the swBoB, *G. glutinata* is associated with eddy-induced productivity during the winter season (Salman and Saraswat, 2024). The muted response of *G. glutinata* suggests that the environmental changes associated with the 4.2 ka event did not substantially alter the ecological niche occupied by *G. glutinata*. However, the high tolerance limit of *G. glutinata* is also evident by its high abundance around canonical 4.2 ka event responding to the peak intensity of the event and suggests a relatively high winter productivity and intensification of the IWM.

*Pulleniatina obliquiloculata* showed a progressive increase and decrease in its abundance throughout the event, reaching its highest abundance during the period of strongest IWM (**Fig. 6; Table 2**). *Pulleniatina obliquiloculata* thrives in subsurface waters at the lower limit of thermocline and is commonly used as a proxy for the changes in thermocline structure (Baohua et al., 1997; Ravelo et al., 1990). Based on the plankton tow studies, *P. obliquiloculata* was suggested to be abundant during the winter season (Ravelo and Fairbanks, 1992; Bé and Tolderlund, 1971). The high abundance of *Pulleniatina obliquiloculata* during 4.2 ka event suggests the deepening of thermocline due to stronger IWM and a weaker ISM. Its abundance pattern closely parallels the increase in WMA, supporting the inference of strengthened winter monsoon conditions during the prolonged 4.2 ka event.

The highest abundance of planktic foraminifera was at ~4.7 ka, just before the onset of the event, after which it decreased gradually until 3.8 ka (**Fig. 6**). The planktic foraminiferal abundance represents annual average response and is not season-specific. Therefore, its abundance can be used only for annual average changes in productivity (Salman and Saraswat, 2024). The gradual decline in TPN therefore reflects a sustained reduction in annual biological production. The progressive nature of this decline is consistent with the two-phase evolution inferred from geochemical proxies, whereby the initial phase was characterized by surface and subsurface hydrographic reorganization and changing organic matter sources, while the later phase witnessed further reduction in productivity and carbon burial.

### 5.3 Monsoon seasonality and productivity changes during the 4.2 ka event

The southwestern Bay of Bengal is strongly influenced by the Indian summer and winter monsoon seasonality (Schott and McCreary, 2001). The planktic foraminifera species flourish during different seasons (Salman and Saraswat, 2024; Maeda et al., 2021; Stoll et al., 2007; Schulz et al., 2002; Guptha et al., 1997). Both the sediment trap and core-top studies across the North Indian Ocean have demonstrated pronounced seasonal variability in both shell flux and spatial distribution of planktic foraminiferal species (Salman and Saraswat, 2024; Maeda et al.,

https://doi.org/10.5194/egusphere-2026-4747
Preprint. Discussion started: 1 September 2026


2022; Bhadra and Saraswat, 2021; Stoll et al., 2007; Schulz et al., 2002; Guptha et al., 1997). The strong monsoon seasonality in the swBoB drives marked contrast in sea surface temperature, salinity, and nutrient availability (Schott and McCreary, 2001). Since these hydrographic parameters exert direct control on planktic foraminiferal abundance and species composition, individual species can serve as sensitive indicators of seasonal oceanographic change. Therefore, the summer and winter monsoon assemblages of planktic foraminifera were used to understand the past monsoon seasonality.

The planktic foraminiferal assemblage data also indicates that the prolonged 4.2 ka event evolved through two stages (**Fig. 7**). During phase 1, the mean SMA value remained comparable to those during the pre-event interval, although gradual decreasing trend was evident. This suggests that the onset of the event was not marked by an abrupt weakening of the ISM but rather by a progressive reduction in its influence. A pronounced decline in SMA occurred during phase 2, indicating substantial weakening of ISM. Overall, it was relatively low throughout the event from 4.65 ka to 3.97 ka, which confirmed the weakening of the ISM during the prolonged 4.2 ka event. On the other hand, the WMA slightly increased during phase 1 and attained its highest value during phase 2 (**Fig. 7**). The simultaneous decrease in SMA and increase in WMA suggests a progressive shift in monsoon seasonality characterized by weakening ISM and strengthening IWM. The seasonal reorganization of monsoons suggests that the climatic perturbation associated with the prolonged 4.2 ka event involved not only reduced ISM forcing but also enhanced IWM influence over the swBoB.

The reduced marine productivity was closely linked to changes in monsoon seasonality and associated upper-ocean hydrography. In the modern swBoB, Chlorophyll-a concentrations are relatively high during the summer monsoon season and relatively low during the winter season at the core site (**Fig. 2**), indicating that annual biological production is largely controlled by ISM-driven nutrient supply. Although IWM influence increased during the event, as indicated by the increase in WMA abundance, the enhanced IWM was insufficient to offset the reduction in ISM-driven productivity. The strengthened IWM increased freshwater discharge and reduced surface water salinity in the swBoB (Dimri et al., 2016; Kripalani and Kumar, 2004; Khole and De, 2003), consistent with the higher $C_{org}/N$ ratio observed during the event. The higher $C_{org}/N$ ratio can be either due to the higher terrestrial influence and/or preferential degradation of N-rich marine organic matter. Simultaneously, the reduced salinity suppressed the calcification and promoted the formation of lighter foraminiferal shells (Zarkogiannis et al., 2022; Trask, 1938), thereby contributing to lower $CaCO_3$ accumulation despite of the persistence of winter productivity. A majority of te planktic foraminiferal species attain their maximum flux during the summer season (Salman and Saraswat, 2024; Maeda et al., 2022; Guptha et al., 1997). Therefore, the progressive weakening of the ISM exerted a disproportionately larger influence on the annual productivity than the strengthening IWM. Consequently, the two-step reduction in marine productivity during the prolonged 4.2 ka event reflects not only a decline in nutrient supply associated with a weaker ISM but also a shift towards a more winter monsoon-dominated hydrographic condition that favored terrestrial influence, organic matter degradation, and reduced carbonate production.

The *G. bulloides*/*G. ruber* ratio did not change at 4.65 ka but increased sharply at 4.45 ka, coincident with the abrupt decline in *G. ruber* abundance (**Fig. 7**). In many settings, higher *G. bulloides*/*G. ruber* ratio is interpreted as evidence of enhanced productivity or sea surface cooling (Singh et al., 2011; Toledo et al., 2008; Anand et al., 2008). However, in our record, the productivity signal is inconsistent with the simultaneous decrease in CF, TPN, $CaCO_3$, $C_{org}$, and N observed during the event. Instead, the increase in the ratio appears to be primarily driven by the decrease in *G. ruber* rather than an increase in *G. bulloides* abundance. The temperature and salinity have a major control on *G. ruber* as it preferentially inhabits warm and stratified upper water column conditions (Salman and Saraswat, 2024; Saraswat et al., 2023; Yadav et al., 2022; Anand et al., 2008). Therefore, the decrease in its abundance during Phase 2 indicates sea surface cooling and a less stratified upper ocean. However, the decrease in *G. bulloides* was not as prominent as that observed in *G. ruber* throughout the event. Therefore, the higher *G. bulloides*/*G. ruber* ratio is interpreted as an indicator of cooler and less stratified surface water conditions rather than enhanced productivity.

The monsoon indicator planktic foraminiferal assemblages suggest that the prolonged 4.2 ka event was characterized by two step weakening of ISM and strengthening of IWM. The concurrent changes in summer and winter monsoons that influenced the upper water column structure, terrigenous dilution, marine productivity and carbon burial, highlight the central role of monsoon seasonality in regulating oceanographic conditions and carbon cycling in the swBoB during the prolonged 4.2 ka event.

### 5.4 Regional response of monsoon and carbon burial to the 4.2 ka event

Globally, the climatic response to the 4.2 ka event varies at decadal scales due to regional propagation of climatic signals and the differing sensitivity of various proxy archives (Railsback et al., 2018). The discrepancy in timing across records is further attributed to differences in proxy resolution and chronological diachrony, compounded by age uncertainties of up to several centuries in most records. Despite these limitations, the event has been reported

https://doi.org/10.5194/egusphere-2026-4747
Preprint. Discussion started: 1 September 2026


from various parts of the Indian subcontinent and the North Indian Ocean using diverse proxy archives, although the precise beginning, termination, and duration could not be ascertained at many locations due to poor temporal resolution. Nevertheless, a majority of these records consistently suggest a shift in monsoon intensity during the 4.2 ka event (Saraswat et al., 2023a, 2016; Shah et al., 2022; Laskar and Bohra, 2021; Giosan et al., 2018; Bhushan et al., 2018; Sandeep et al., 2017; Kathayat et al., 2017; Berkelhammer et al., 2012; Dixit et al., 2014, 2018; Prasad et al., 2014; Staubwasser et al., 2003; Kudrass et al., 2001). A recent Hemispheric synthesis of 200 high-quality paleoclimate records further corroborates this regional drying signal, demonstrating that the South Asian region shows one of the highest hydroclimatic excursion during the 4.2 ka event among all Northern Hemisphere regions examined (Nan et al., 2025). A prominent decrease in $C_{org}$ and $CaCO_3$ (%) from its mean state value between 4.6 and 4.1 ka in the Gulf of Mannar (SSD004 GC02) (**Fig. 8a & b**) indicates a decrease in carbon burial due to a weaker ISM (Saraswat et al., 2023a). A similar study from the offshore of Pennar River (Suokhrie and Saraswat, 2024; SK308 GC02) also reported a decrease in $C_{org}$ and $CaCO_3$ (**Fig. 8a & b**), marking a significant impact of the 4.2 ka event in wBoB and GoM, which led to the decrease in carbon burial.

The decrease in $C_{org}$ and $C_{org}$/N ratio between 4.5-4.2 ka from the Lonar Lake (**Fig. 8b**) suggests the beginning of ISM weakening at 4.5 ka instead of 4.2 ka in central India (Prasad et al., 2014). The decrease in $CaCO_3$ (%) at 4.65 ka in the Dahar Lake (**Fig. 8a**), northwestern India, suggests a gradual change in precipitation while the enriched $\delta^{18}O$ of gastropods implies an intense weakening in the ISM at 4.1 ka (Dixit et al., 2014). Collectively, these records point to a diachronous but widespread decrease in ISM intensity because these sites are largely affected by the summer monsoon. The planktic foraminiferal assemblages in our record suggested a two-step weakening in ISM and strengthening of IWM, which led to a decrease in carbon burial beginning at 4.65 ka and continuing until 3.97 ka (**Fig. 4 & 7**). Despite minor differences in the precise timing and duration of the event across individual records, the concurrent shift in monsoon intensity and carbon burial recorded in both the marine and terrestrial archives confirms the widespread impact of the 4.2 ka event across the North Indian Ocean and Indian subcontinent.

The change in the relative abundance of *G. bulloides* remained relatively stable during pre-event and phase 1, whereas it decreased abruptly during phase 2 suggesting a major weakening in ISM that occurred at 4.45 ka during phase 2 (**Fig. 8d**). *Globigerina bulloides* exhibited a less discernible response to the ISM in Gulf of Mannar during the 4.2 ka event (**Fig. 8d**; SSD004 GC02). However, a decrease in *G. bulloides* offshore Pennar River suggests a weaker ISM between 4.6 and 4.1 ka (**Fig. 8d**; SK308 GC02). A very prominent drop in *G. bulloides* abundance at 4.65 ka in the eastern Arabian Sea (Saravanan et al., 2019; SK291 GC15) corresponds well with the onset of prolonged 4.2 ka event recorded in SSD067 PC03, further confirming the weakening of ISM during this interval. In our record, *P. obliquiloculata* and WMA indicated a strong IWM in the swBoB. The high abundance of *G. falconensis* in the northeastern Arabian Sea (neAS) also suggests a stronger IWM around 4.2 ka event (Schulz et al., 2002). Schulz et al. (2002) linked the higher abundance of *G. falconensis* to strong vertical mixing due to a strong IWM. However, there was a gradual decrease in IWM also towards the 3.97 ka. Therefore, both Indian summer and winter monsoon were relatively weaker towards the end of the event at ~4.05 ka. This transition coincides well with the termination of the mature phase of the Indus civilization (Khan et al., 2024; Dixit et al., 2014; Berkelhammer et al., 2012; Staubwasser et al., 2003).

Interestingly, around 4.6 ka, a cooling phase began with a moderate temperature decline at 4.4 ka, followed by a more pronounced SST decrease of ~1°C between 4.2 ka and 3.8 ka in the northern Arabian Sea (Burdanowitz et al., 2020). Foraminiferal record from the same core indicates reduced Indus River discharge and increased winter monsoon mixing between 4.5 ka and 4.25 ka (Giesche et al., 2019; Staubwasser et al., 2003). The lower SST and declining fluvial input persisted until approximately 3.0 ka. This cooling trend between 4.6 and 3.0 ka has been recorded from the Arabian Sea and the Indian subcontinent (Gaye et al., 2018; Zhao et al., 2017). The temperature dropped from 28.8°C to 27.7°C in the seAS between 4.8 ka and 4.2 ka, accompanied by a depletion in $\delta^{18}O_{sw\text{-}ivc}$ from 0.4 to 0.14‰ between 4.4 ka and 3.6 ka (Saraswat et al., 2016). The depleted $\delta^{18}O_{sw\text{-}ivc}$ values close to 4.2 ka event point towards an intensification of monsoon (Saraswat et al., 2016). However, the enhanced advection of low salinity waters from the Bay of Bengal may have contributed to the depleted $\delta^{18}O_{sw\text{-}ivc}$ signal around 4.2 ka in the seAS. The concurrent cooling during the 4.2 ka event and a stronger winter monsoon, as indicated by WMA, may have led to strong EICC and WMC, which likely facilitated a greater transport of low salinity waters from the Bay of Bengal into the seAS.

From the swBoB, Suokhrie and Saraswat (2024) reported enriched $\delta^{18}O_{G.\ ruber}$ at 4.45 ka to 4.1 ka (**Fig. 8e**; SK308 GC02). Similarly, from the west-central Bay of Bengal (NGHP-01-16A), Ponton et al. (2012) also reported enriched $\delta^{18}O_{G.\ ruber}$ between 4.25 ka to 4.0 ka suggesting a weaker ISM during the second phase of the event. Although a centennially resolved record (Kudrass et al., 2001) from the northern Bay of Bengal (SO93-126KL) contradicts this by suggesting depleted $\delta^{18}O$ values between 4.6 ka and 4.0 ka (**Fig. 8e**). The

https://doi.org/10.5194/egusphere-2026-4747
Preprint. Discussion started: 1 September 2026


depleted $\delta^{18}O$ implies increased precipitation or riverine influx due to intense monsoon. However, the weaker ISM during the 4.2 ka event, has been reported from various parts of the North Indian Ocean (Laskar and Bohra, 2021; Staubwasser et al., 2003). Therefore, the $\delta^{18}O$ should be enriched if the ISM was weaker, as it is well known that the northern Bay of Bengal receives a huge monsoonal flux during the summer season (Akhil et al., 2014). Therefore, it remains debatable why the salinity was low between 4.6 ka and 4.0 ka. However, the timing of the shift in $\delta^{18}O$ is well aligned with the onset and termination of the event as observed in this study.

The heavier $\delta^{18}O$ of a gastropod species at 4.2 to 4.0 ka from the Kotla Dahar Lake recorded a weaker ISM around canonical 4.2 ka event (**Fig. 8e**). Furthermore, a speleothem record from the Mawmluh Cave (KM-A) pointed to the initiation of the event at 4.3 ka, with extreme drought between 4.05 to 3.9 ka (**Fig.** 8e), suggesting the major weakening of ISM during the phase 2 of the 4.2 ka event. However, James et al. (2025) noted that only this single record is not sufficient to explain the broader Asian monsoon shift, as the isotopic excursion observed at Mawmluh cave was not replicated in most other speleothem records from the region. Nevertheless, the two-step weakening of the ISM recorded in our swBoB core with a moderate decline during Phase 1 (4.65-4.45 ka) followed by a more pronounced weakening during Phase 2 (4.45-3.97 ka) is broadly consistent with the two-phase evolution of arid conditions synthesized by Nan et al. (2025) across the South Asian region. This two-phase hydroclimate trajectory, reconstructed from 12 high-quality South Asian proxy records with a 70.6% excursion incidence (Nan et al., 2025), reinforces our planktic foraminiferal and geochemical evidence and suggests that the limitations of individual speleothem records noted by James et al. (2025) do not undermine the broader regional signal when multi-proxy marine and terrestrial archives are considered collectively. In our record, phase 1 represents a moderate initial ISM weakening, while phase 2 captures a more pronounced and sustained monsoon decline accompanied by IWM strengthening. The ISM weakening during phase 2 encompasses both the development phase (4.3-4.1 ka) and the amplification phase (4.1-3.9 ka), mechanistically consistent with the progressive amplification proposed by Nan et al. (2025). The early onset of Phase 1 at 4.65 ka is not anomalous, as precursor signals of the 4.2 ka event as early as 4.5-4.6 ka have been reported in several records (McKay et al., 2024; Railsback et al., 2018), including the North Indian Ocean (Saravanan et al., 2019; Burdanowitz et al., 2020; Saraswat et al., 2023a, 2016). Therefore, the event window (4.65 -3.97 ka) in our record suggests that the swBoB captured an early and spatially proximal expression of climate and monsoon reorganization during the prolonged 4.2 ka event.

https://doi.org/10.5194/egusphere-2026-4747
Preprint. Discussion started: 1 September 2026


The findings of McKay et al. (2024) and Nan et al. (2025) provide important yet contrasting contexts for the ongoing debate on the global versus regional significance of the 4.2 ka event. McKay et al. (2024) concluded that excursions during the 4.2 ka event do not occur in large or coherent spatial regions, rendering it comparable to background Holocene variability. However, this assessment is likely influenced by the aggregation of opposing wet and dry signals across climatically distinct sub-regions, causing dipole-structured hydroclimate responses to cancel each other statistically and producing an apparent null result (Nan et al., 2025). The Europe circum-Mediterranean (ECM) region exhibits a "northern wet, southern drought" dipole; the East Asian monsoon (EAM) region shows an opposing "northern drought, southern wet" structure, and the North American (NA) region displays an East-West dipole, all driven by systematic shifts in the westerly jet and monsoon rain belt (Nan et al., 2025; Li et al., 2019; Chen et al., 2015; Sun et al., 2017; Wu et al., 2019). Notably, McKay et al. (2024) themselves acknowledge that regional excursions during this interval were real and potentially impactful, consistent with the coherent arid signal documented across South Asia. In the South Asian region, no dipole structure exists and drying is the dominant signal (Nan et al., 2025). The multi-proxy evidence presented here, spanning marine sediments from the North Indian Ocean to terrestrial records from Indian (**Fig. 8**), is consistent with this South Asian arid signal and confirms the widespread impact of the 4.2 ka event across the Indian subcontinent. Rather than contradicting the findings of McKay et al. (2024), our results reinforce their observation that regional excursions were real and impactful, while supporting the argument given by Nan et al. (2025) that the event shows spatial heterogeneity, not its absence, which is the defining characteristic of the 4.2 ka event, marking a fundamental shift in monsoon seasonality at the Northgrippian-Meghalayan age boundary.

### 5.5 Driving mechanism of the prolonged 4.2 ka event

The driving mechanisms of the 4.2 ka event in the Indian monsoon region reflect a complex interplay of North Atlantic Ocean-atmosphere forcing, ITCZ migration, Indo-Pacific ENSO forcing, IOD variability, and insolation changes operating across different timescales. The solar forcing has often been linked to variation in Indian monsoon intensity on a millennial to multi-centennial scale. The small insolation change caused a large variation in precipitation throughout the Holocene (Thamban et al., 2007). The seasonal insolation in the Northern Hemisphere significantly changed before the onset of the Maghalayan Age (Burdanowitz et al., 2020). On a millennial scale, the gradual decrease in Northern Hemisphere summer insolation from ~6.3 ka onward progressively shifted the summer ITCZ southward, reducing the ISM

https://doi.org/10.5194/egusphere-2026-4747
Preprint. Discussion started: 1 September 2026


precipitation (Fleitmann et al., 2007). The seasonal migration of ITCZ controls the duration, termination, and amount of precipitation during the summer and winter monsoon seasons in the tropical and subtropical regions (Geen et al., 2020). Generally, the ITCZ migrates towards the warm hemisphere on seasonal and longer timescales (Schneider et al., 2014). The long-term shift in the duration of summer season was observed at 4.5 ka onwards (Fleitmann et al., 2007), coinciding with the onset of the weaker ISM phase. The decrease in Northern Hemisphere summer insolation progressively shifted the summer ITCZ, reducing summer monsoon precipitation over the South Asian region. Concurrently, the increase in winter insolation strengthened the winter monsoon on orbital timescales (Burdanowitz et al., 2020), consistent with the SMA and WMA of planktic foraminifera in our record suggesting a weaker ISM and stronger IWM between 4.65 and 3.97 ka (**Fig. 7**). However, there was no abrupt shift in ITCZ at 4.65 ka. The progressive nature of insolation changes from the middle Holocene onward (Saraswat et al., 2016; Fleitmann et al., 2007), without any abrupt shift around 4.2 ka event, suggests that orbital forcing alone cannot explain the abrupt shift in monsoon seasonality during the 4.2 ka event documented in our record. Additional forcing mechanisms operating on shorter timescales are therefore required to explain the observed monsoon reorganization.

In addition to orbital-scale insolation forcing, both Ocean-atmosphere coupled phenomena such as ENSO, IOD variability, ITCZ migration, and North Atlantic Ocean-atmosphere forcing, could have contributed to the abrupt climatic shift during the 4.2 ka event (Helama, 2024; Booth et al., 2005; Staubwasser et al., 2003). A weaker AMOC reduces the northward transport of warm, saline surface waters from the tropics to high latitudes, leading to a cooling of the North Atlantic and adjacent Northern Hemisphere landmasses (Hoogakker et al., 2011; Sejrup et al., 2011). This high-latitude cooling diminishes the interhemispheric thermal gradient, which in turn drives a southward displacement of the ITCZ and the associated tropical rain belt (Liu et al., 2020; Stouffer et al., 2006; Zhang and Delworth, 2005). Over the Indian subcontinent, this AMOC induced cooling further reduces the land-sea thermal contrast between the Asian landmass and the Indian Ocean, weakening the pressure gradient that drives moisture-laden southwesterly winds onshore during the summer monsoon season (Naidu et al., 2020; Lu et al., 2006). Although, the high-resolution $^{231}Pa/^{230}Th$ records from the western North Atlantic Ocean suggested limited AMOC variability, at ODP site 1063, about 15% weakening of AMOC coincides with 4.2 ka event (Gerber et al., 2025). However, with a minor deviation during the studied interval, it maintains consistency with the two-step decrease in SMA, $CaCO_3$, $C_{org}$ and increase in WMA with the slowdown of AMOC during the phase 1 and phase 2 of the prolonged 4.2 ka event (**Fig. 9**). A relatively high $C_{org}$ content during phase 1

https://doi.org/10.5194/egusphere-2026-4747
Preprint. Discussion started: 1 September 2026


was due to the increased terrestrial contribution of organic matter as suggested by higher $C_{org}/N$ ratio. Another record based on sortable silt content (10-63 µm) from the Northeast and Northwest Atlantic Ocean suggested a long-term decrease in flow speed of northeast Atlantic deep water after 6.5 ka (Hoogakker et al., 2011). The deviation in z-score, considering the mean Holocene background state of AMOC, further suggested a two-step weakening in AMOC strength during phase 1 and phase 2 of the prolonged 4.2 ka event (**Fig. 9**). The recent hemispheric-scale proxy synthesis and model simulation by Nan et al. (2025) suggested North Atlantic Ocean-atmosphere forcing as the primary trigger of the 4.2 ka event. Specifically, a weakening of AMOC at ~4.4 (Hoogakker et al., 2011), a transition to a negative Atlantic multi-decadal oscillation (AMO) like pattern at ~4.3 ka (Sejrup et al., 2011), and a positive North Atlantic oscillation (NAO) like pattern during the event (Olsen et al., 2012) collectively initiated the development phase of the 4.2 ka event. The North Atlantic forcing is directly relevant to ISM weakening through two well established pathways. First, a negative AMO like pattern decreases the thermal contrast between Asian landmasses and Indian Ocean, reducing the land-sea temperature gradient that drives ISM (Naidu et al., 2020; Lu et al., 2006). Second, a weaker AMOC induces a southward shift of ITCZ, further diminishing ISM precipitation (Liu et al., 2020; Stouffer et al., 2006; Zhang and Delworth, 2005). Both pathways are consistent with moderate ISM weakening observed in our record during phase 1, which predates the canonical 4.3 ka onset of the development phase and likely reflects the early sensitivity of the swBoB to initial North Atlantic forcing signal transmitted through ISM system. It is also important to note that, unlike the 8.2 ka event, which is robustly attributed to a freshwater-forced slowdown of AMOC, the 4.2 ka event lacks a comparably clear large-scale freshwater forcing (Gerber et a., 2025). Nevertheless, the regionally coherent reconstruction of AMOC weakening from the North Atlantic (Hoogakker et al., 2011) and its consistency with the hemispheric scale proxy synthesis (Nan et al., 2025), combined with mechanistic teleconnections, provide reasonable support for invoking AMOC weakening, as a driver of the shift in monsoon seasonality documented in our record.

In the eastern Pacific Ocean, both the intensity and frequency of ENSO events per 100 years decreased in two steps at 4.65 ka during phase 1 and again at ~4.4 ka during phase 2, and continued until 4.05 ka (Moy et al., 2002; **Fig. 9**). El Niño, La Niña, and associated Southern Oscillation in the equatorial Pacific Ocean strongly affect the Indian monsoon (Ratna et al., 2024). During the El Niño (warm phase), Indian subcontinent experiences drought conditions, while during the La Niña (cool phase), it receives extensive rainfall (Ratna et al., 2024). The

https://doi.org/10.5194/egusphere-2026-4747
Preprint. Discussion started: 1 September 2026


ENSO activity increases with the warming (Latif and Keenlyside, 2009). The 4.2 ka event was a cold phase in the low to mid-latitude regions (Railsback et al., 2018). Therefore, the low ENSO activity due to cooling in the low latitude regions suggests its response to the cooling triggered by North Atlantic forcing, not a driver of the 4.2 ka event. If ENSO has acted as a driving mechanism, it would have strengthened the ISM during the 4.2 ka event. A study from the South China Sea, a region influenced by both the summer and winter monsoons, also suggested that the warm phase of ENSO was weaker while the cold phase was stronger during the 4.2 ka event (Dang et al., 2020). The cold phase (La Niña) was associated with winter season, which led to the stronger winter monsoon during the 4.2 ka event. The transition from a La Niña like pattern to an El Niño like pattern in the equatorial Pacific at ~4.1 ka (Conroy et al., 2008; Moy et al., 2002; Haug et al., 2001) significantly amplified the impact of the 4.2 ka event at the end of phase 2. Our record also suggest that both the Indian summer and winter monsoons were relatively weaker at ~4.05 ka. Therefore, the two-phase structure of ISM weakening and IWM strengthening documented in our record is mechanistically consistent with the sequential influence of North Atlantic forcing during Phase 1 and Phase 2, followed by the combined amplification of North Atlantic and Pacific El Niño like forcing at the end of Phase 2.

The positive IOD phase starts with the cooling in the southeastern tropical Indian Ocean (STIO) and warming of the western tropical Indian Ocean (WTIO) in May – June while negative IOD phase starts with warm STIO and cool WTIO in December – January (Brown et al., 2009; Saji et al., 1999). A strong positive IOD phase causes heavy rainfall over east Africa and Indian subcontinent (Saji et al., 1999). However, at the same time, the strong El Nino phase may cause drought conditions over the Indian subcontinent (Brown et al., 2009). During the early-middle Holocene, the weak IOD variability was associated with strengthened monsoon when the ENSO activity was suppressed while strong IOD variability was associated with weaker monsoon during the late Holocene when ENSO events were more frequent (Brown et al., 2009; Abram et al., 2007). Although direct high-resolution IOD records spanning the 4.2 ka event are currently unavailable, the established Holocene-scale relationship between IOD variability and ENSO activity (Brown et al., 2009; Abram et al., 2007) allows for an indirect inference regarding IOD behavior during this period. Following these early and late Holocene analogues, we suggest a positive relation between ENSO and IOD variability. Therefore, the reduction in ENSO activity during the 4.2 ka event is inferred as a weakening of IOD variability, which further reinforced the ISM weakening in our record. Further high-resolution reconstructions spanning the 4.2 ka event are needed to directly test this hypothesis.

https://doi.org/10.5194/egusphere-2026-4747
Preprint. Discussion started: 1 September 2026


The rate of global sea-level rise was increasing continuously throughout the studied interval and slowed down between 4.5 and 4.1 ka (Grant et al., 2014; **Fig. 9**). However, the regional sea level was relatively higher than the present sea level between 4.4 and 4.1 ka. Subsequently, it was below the present sea level after 4.10 ka along the east and west coasts of India (Das et al., 2022; Loveson and Nigam, 2019). Therefore, the sea level changes during the 4.2 ka event may not have much influence on the organic and inorganic carbon burial in the swBoB. The summer and winter monsoons primarily influenced it. The confluence of North Atlantic forcing, ITCZ shifting, ENSO-IOD variability, and insolation changes collectively drove the prolonged shift in Indian monsoon seasonality and carbon burial decrease in the swBoB at the Northgrippian-Meghalayan age boundary.

## 6. Conclusions

We provide decadal-scale insights into the complex interaction between climatic factors and seasonal monsoon dynamics during the 4.2 ka event. The 4.2 ka event evolved in two phases, beginning at 4.65 ± 0.17 ka and persisted until 3.97 ± 0.18 ka, with a duration of 680 years in the Bay of Bengal. The event exhibited diachrony in its onset and duration across different records but resulted in a significant decrease in carbon burial. Phase 1 was characterized by a decrease in inorganic and an increase in organic carbon due to increased terrestrially derived organic matter contribution, as evidenced by a high $C_{org}/N$ ratio, while phase 2 was characterized by sustained reduction in both inorganic and organic carbon burial. The synchronous decrease in coarse fraction, $CaCO_3$, organic carbon, nitrogen, and individual species of planktic foraminifera indicated a progressive decrease in marine productivity during phase 1 and phase 2 of the 4.2 ka event. The seasonal shift in the Indian monsoon was a key driver in reducing the marine productivity and carbon burial during the prolonged 4.2 ka event. The individual planktic foraminifera species and their summer and winter monsoon assemblages suggest that the seasonal behavior of the Indian monsoon evolved in two stages, namely phase 1 that was characterized by a stronger but gradually weakened ISM, accompanied by a moderate strengthening of IWM, and phase 2 that was marked by a pronounced weakening of ISM and strengthening of IWM. Towards the termination of the event at ~4.05 ka, both summer and winter monsoons weakened simultaneously, coinciding with the collapse of the mature phase of the Indus Valley Civilization. The AMOC weakening and its associated North Atlantic Ocean-atmosphere forcing triggered the 4.2 ka event with a complex interaction of seasonal insolation changes, southward ITCZ shift, weak ENSO activity, and IOD variability were the major factors driving the prolonged 4.2 ka event. The

https://doi.org/10.5194/egusphere-2026-4747
Preprint. Discussion started: 1 September 2026


findings from this study and comparison with previous records on the 4.2 ka event confirms its occurrence and climatic impacts across the Indian subcontinent and the North Indian Ocean.

## Acknowledgment

We thank the Director, CSIR-National Institute of Oceanography, Goa, India for the infrastructure support and permission to publish the findings. This work was supported by the Science and Engineering Research Board, Department of Science and Technology, Government of India, under Core Research Grant Scheme to RS (Grant Number CRG/2019/000221). Authors are thankful to all the crew members and scientists who took part in 67th cruise of RV *Sindhu Sadhana* (SSD076). A special thanks to the Ship Cell technical officers of the National Institute of Oceanography, Goa, for their assistance in operating the piston corer. We also appreciate the help provided by Mrs. Teja Ankush Naik in carbon and nitrogen analysis under the Central Analytical Facility (CAF) of the CSIR-National Institute of Oceanography, Goa, India. Authors thank Dr. Pankaj Kumar and Dr. Rajveer Sharma for the help in radiocarbon analysis at the Inter-University Accelerator Center, New Delhi, India. MS Acknowledges the Joint CSIR-University Grants Commission for the research fellowship.

## Data availability statement

The authors declare that the data supporting the findings of this study is available within the manuscript and in its supplementary information files.

## Authors contribution

**Mohd Salman:** Conceptualization, methodology, investigation, sample processing, data curation, formal analysis, visualization, interpretation of results, and writing original draft.
**Rajeev Saraswat:** Conceptualization, supervision, methodology, resources, interpretation of results, review, and editing.

## Competing interest

The authors declare that they have no conflict of interest.

https://doi.org/10.5194/egusphere-2026-4747
Preprint. Discussion started: 1 September 2026


# References

Abram, N. J., Gagan, M. K., Liu, Z., Hantoro, W. S., McCulloch, M. T., & Suwargadi, B. W. (2007). Seasonal characteristics of the Indian Ocean Dipole during the Holocene epoch. *Nature*, 445, 299-302.

Ahmad Shah, R., Khan, I., Rahman, A., Kumar, S., Achyuthan, H., Shukla, A.D., Kumar, P. & Dash, C. (2022). Holocene climate events and associated land use changes in the eastern coast of India: Inferences from the Chilika Lagoon. *The Holocene*, 32, 1081-1090.

Akhil, V. P., F. Durand, M. Lengaigne, J. Vialard, M. G. Keerthi, V. V. Gopalakrishna, C. Deltel, F. Papa, and C. de Boyer Montegut (2014), A modeling study of the processes of surface salinity seasonal cycle in the Bay of Bengal. *Journal of Geophysical Research: Oceans*, 119, 3926–3947.

Alappat, L., Tsukamoto, S., Singh, P., Srikanth, D., Ramesh, R., & Frechen, M. (2010). Chronology of Cauvery delta sediments from shallow subsurface cores using elevated-temperature post-IR IRSL dating of feldspar. *Geochronometria*, 37, 37-47.

Anand, P., Kroon, D., Singh, A. D., Ganeshram, R. S., Ganssen, G., & Elderfield, H. (2008). Coupled sea surface temperature–seawater δ18O reconstructions in the Arabian Sea at the millennial scale for the last 35 ka. *Paleoceanography*, 23, PA4207.

Ankit, Y., Kumar, P., Anoop, A., Mishra, P. K., & Varghese, S. (2017). Mid-late Holocene climate variability in the Indian monsoon: Evidence from continental shelf sediments adjacent to Rushikulya river, eastern India. *Quaternary International*, 443, 155-163.

Banakar, V. K., Baidya, S., Shankar, D., Nanjundiah, R. S., & Jain, V. (2022). Possible zonal asymmetry of the Indian summer monsoon rainfall after ~5 ka BP as revealed by paleo-salinity in the eastern Arabian Sea. *Journal of Earth System Science*, 131, 161.

Banerji, U. S., Arulbalaji, P., & Padmalal, D. (2020). Holocene climate variability and Indian Summer Monsoon: an overview. *The Holocene*, 30, 744-773.

Baohua, L., Zhimin, J., & Pinxian, W. (1997). Pulleniatina obliquiloculata as a paleoceanographic indicator in the southern Okinawa Trough during the last 20,000 years. *Marine Micropaleontology*, 32, 59-69.

Bé, A. W. H., & Tolderlund, D. S. (1971). Distribution and ecology of living planktonic foraminifera in surface waters of the Atlantic and Indian Oceans. *The micropaleontology of oceans*, 105-149.

Berkelhammer, M., Sinha, A., Stott, L., Cheng, H., Pausata, F. S., & Yoshimura, K. (2012). An abrupt shift in the Indian monsoon 4000 years ago. *Climates, landscapes, and civilizations*, 198, 75-88.

Bhadra, S. R., & Saraswat, R. (2021). Assessing the effect of riverine discharge on planktic foraminifera: A case study from the marginal marine regions of the western Bay of Bengal. *Deep Sea Research Part II: Topical Studies in Oceanography*, 183, 104927.

Bhushan, R., Sati, S. P., Rana, N., Shukla, A. D., Mazumdar, A. S., & Juyal, N. (2018). High-resolution millennial and centennial scale Holocene monsoon variability in the Higher Central Himalayas. *Palaeogeography, Palaeoclimatology, Palaeoecology*, 489, 95-104.

Booth, R. K., Jackson, S. T., Forman, S. L., Kutzbach, J. E., Bettis Iii, E. A., Kreigs, J., & Wright, D. K. (2005). A severe centennial-scale drought in midcontinental North America 4200 years ago and apparent global linkages. *The Holocene*, 15, 321-328.

Brown, J., Lynch, A. H., & Marshall, A. G. (2009). Variability of the Indian Ocean Dipole in coupled model paleoclimate simulations. *Journal of Geophysical Research: Atmospheres*, 114 (D11).

Burdanowitz, N., Rixen, T., Gaye, B., & Emeis, K. C. (2020). Holocene climatic changes in the Westerly-Indian Monsoon realm and its anthropogenic impact. *Climate of the Past Discussions*, 2020, 1-22.

https://doi.org/10.5194/egusphere-2026-4747
Preprint. Discussion started: 1 September 2026


Chen, J., Chen, F., Feng, S., Huang, W., Liu, J., & Zhou, A. (2015). Hydroclimatic changes in China and surroundings during the Medieval Climate Anomaly and Little Ice Age: spatial patterns and possible mechanisms. *Quaternary Science Reviews*, 107, 98-111.

Chen, X., Pan, D., Bai, Y., He, X., Chen, C. T. A., & Hao, Z. (2013). Episodic phytoplankton bloom events in the Bay of Bengal triggered by multiple forcings. *Deep Sea Research Part I: Oceanographic Research Papers*, 73, 17-30.

Conroy, J. L., Overpeck, J. T., Cole, J. E., Shanahan, T. M., & Steinitz-Kannan, M. (2008). Holocene changes in eastern tropical Pacific climate inferred from a Galápagos lake sediment record. *Quaternary Science Reviews*, 27 (11-12), 1166-1180.

Cullen, H. M., Demenocal, P. B., Hemming, S., Hemming, G., Brown, F. H., Guilderson, T., & Sirocko, F. (2000). Climate change and the collapse of the Akkadian empire: Evidence from the deep sea. *Geology*, 28, 379-382.

Cullen, J. L., & Prell, W. L. (1984). Planktonic foraminifera of the northern Indian Ocean: distribution and preservation in surface sediments. *Marine Micropaleontology*, 9 (1), 1-52.

Da Silva, R., Mazumdar, A., Mapder, T., Peketi, A., Joshi, R.K., Shaji, A., Mahalakshmi, P., Sawant, B., Naik, B.G., Carvalho, M.A. & Molletti, S.K. (2017). Salinity stratification controlled productivity variation over 300 ky in the Bay of Bengal. *Scientific reports*, 7 (1), 14439.

Dai, L., Cheng, T. F., Wang, B., & Lu, M. (2023). Subseasonal features of the Indian monsoon. *Journal of Climate*, 36 (20), 7199-7211.

Dang, S., Yu, K., Tao, S., Han, T., Zhang, H., & Jiang, W. (2020). El Niño/Southern Oscillation during the 4.2 ka event recorded by growth rates of corals from the North South China Sea. *Acta Oceanologica Sinica*, 39, 110-117.

Das, A., Sodhi, A., Vedpathak, C.D., Prizomwala, S.P., Agnihotri, R., Makwana, N., Joseph, J., Patel, N., Chopra, S. and Ravi Kumar, M. (2022). Evidence for seawater retreat with advent of Meghalayan era (~ 4200 a BP) in a coastal Harappan settlement. *Geochemistry, Geophysics, Geosystems*, 23 (6), e2021GC010264.

Dimri, A. P., Yasunari, T., Kotlia, B. S., Mohanty, U. C., & Sikka, D. R. (2016). Indian winter monsoon: Present and past. *Earth-science reviews*, 163, 297-322.

Dixit, Y., & Tandon, S. K. (2016). Hydroclimatic variability on the Indian subcontinent in the past millennium: review and assessment. *Earth-Science Reviews*, 161, 1-15.

Dixit, Y., Hodell, D. A., & Petrie, C. A. (2014). Abrupt weakening of the summer monsoon in northwest India~ 4100 yr ago. *Geology*, 42 (4), 339-342.

Dixit, Y., Hodell, D.A., Giesche, A., Tandon, S.K., Gázquez, F., Saini, H.S., Skinner, L.C., Mujtaba, S.A., Pawar, V., Singh, R.N. & Petrie, C.A. (2018). Intensified summer monsoon and the urbanization of Indus Civilization in northwest India. *Scientific reports*, 8 (1), 4225.

Dutt, S., Gupta, A. K., Wünnemann, B., & Yan, D. (2018). A long arid interlude in the Indian summer monsoon during~ 4,350 to 3,450 cal. yr BP contemporaneous to displacement of the Indus valley civilization. *Quaternary International*, 482, 83-92.

Enzel, Y., Ely, L.L., Mishra, S., Ramesh, R., Amit, R., Lazar, B., Rajaguru, S.N., Baker, V.R. and Sandler, A. (1999). High-resolution Holocene environmental changes in the Thar Desert, northwestern India. *Science*, 284 (5411), 125-128.

Fleitmann, D., Burns, S. J., Mudelsee, M., Neff, U., Kramers, J., Mangini, A., & Matter, A. (2003). Holocene forcing of the Indian monsoon recorded in a stalagmite from southern Oman. *Science*, 300 (5626), 1737–1739.

Fleitmann, D., Burns, S.J., Mangini, A., Mudelsee, M., Kramers, J., Villa, I., Neff, U., Al-Subbary, A.A., Buettner, A., Hippler, D. and Matter, A. (2007). Holocene ITCZ and Indian monsoon dynamics recorded in stalagmites from Oman and Yemen (Socotra). *Quaternary Science Reviews*, 26 (1-2), 170-188.

https://doi.org/10.5194/egusphere-2026-4747
Preprint. Discussion started: 1 September 2026


Gadgil, S., & Gadgil, S. (2006). The Indian monsoon, GDP and agriculture. *Economic and political weekly*, 4887-4895.

Gautam, P. K., Narayana, A. C., Kumar, P. K., Bhavani, P. G., Yadava, M. G., & Jull, A. J. T. (2021). Indian monsoon variability during the last 46 kyr: isotopic records of planktic foraminifera from southwestern Bay of Bengal. *Journal of Quaternary Science*, 36 (1), 138-151.

Gaye, B., Böll, A., Segschneider, J., Burdanowitz, N., Emeis, K. C., Ramaswamy, V., Lahajnar, N., Lückge, A., Rixen, T. (2018). Glacial–interglacial changes and Holocene variations in Arabian Sea denitrification. Biogeosciences 15, 507–527.

Geen, R., Bordoni, S., Battisti, D. S., & Hui, K. (2020). Monsoons, ITCZs, and the concept of the global monsoon. Reviews of Geophysics, 58, e2020RG000700.

Gerber, L., Lippold, J., Süfke, F., Valk, O., Testorf, P., Ehnis, M., Tautenhahn, S., Max, L., Chiessi, C.M., Regelous, M. & Szidat, S. (2025). Low variability of the Atlantic Meridional overturning circulation throughout the Holocene. *Nature Communications*, 16 (1), 6748.

Giesche, A., Staubwasser, M., Petrie, C. A., & Hodell, D. A. (2019). Indian winter and summer monsoon strength over the 4.2 ka BP event in foraminifer isotope records from the Indus River delta in the Arabian Sea. *Climate of the Past*, 15 (1), 73-90.

Giosan, L., Orsi, W. D., Coolen, M., Wuchter, C., Dunlea, A. G., Thirumalai, K., Munoz, S. E., Clift, P. D., Donnelly, J. P., Galy, V. & Fuller, D. Q. (2018). Neoglacial climate anomalies and the Harappan metamorphosis. *Climate of the Past*, 14 (11), 1669-1686.

Gomes, H.R., Goes, J.I. and Saino, T., 2000. Influence of physical processes and freshwater discharge on the seasonality of phytoplankton regime in the Bay of Bengal. *Continental Shelf Research*, 20 (3), pp.313-330.

Govil, P., & Naidu, P. D. (2011). Variations of Indian monsoon precipitation during the last 32 kyr reflected in the surface hydrography of the Western Bay of Bengal. *Quaternary Science Reviews*, 30 (27-28), 3871-3879.

Grant, K.M., Rohling, E.J., Ramsey, C.B., Cheng, H., Edwards, R.L., Florindo, F., Heslop, D., Marra, F., Roberts, A.P., Tamisiea, M.E. and Williams, F. (2014). Sea-level variability over five glacial cycles. *Nature communications*, 5(1), 5076.

Gupta, A. K., Anderson, D. M., & Overpeck, J. T. (2003). Abrupt changes in the Asian southwest monsoon during the Holocene and their links to the North Atlantic Ocean. *Nature*, 421 (6921), 354-357.

Gupta, A. K., Anderson, D. M., Pandey, D. N., & Singhvi, A. K. (2006). Adaptation and human migration, and evidence of agriculture coincident with changes in the Indian summer monsoon during the Holocene. *Current Science*, 1082-1090.

Guptha, M. V. S., Curry, W. B., Ittekkot, V., & Muralinath, A. S. (1997). Seasonal variation in the flux of planktic Foraminifera; sediment trap results from the Bay of Bengal, northern Indian Ocean. *The Journal of Foraminiferal Research*, 27 (1), 5-19.

Haug, G. H., Hughen, K. A., Sigman, D. M., Peterson, L. C., & Rohl, U. (2001). Southward migration of the intertropical convergence zone through the Holocene. *Science*, 293 (5533), 1304-1308.

Helama, S. (2024). The 4.2 ka event: A review of palaeoclimate literature and directions for future research. *The Holocene*, 34 (9), 1408-1415

Hemleben, C., Spindler, M., Anderson, O. R. (1989). Modern planktonic Foraminifera. Springer, Berlin

Jacob, J., Chandramohanakumar, N., Jayaraj, K.A., Raveendran, T.V., Balachandran, K.K., Joseph, T., Nair, M., Achuthankutty, C.T., Nair, K.K.C., George, R. and Ravi, Z.P. (2008). Biogeochemistry of the surficial sediments of the western and eastern continental shelves of India. *Journal of Coastal Research*, 24 (5), 1240-1248.

https://doi.org/10.5194/egusphere-2026-4747
Preprint. Discussion started: 1 September 2026


Jagadeesan, L., Jyothibabu, R., Anjusha, A., Mohan, A. P., Madhu, N. V., Muraleedharan, K. R., & Sudheesh, K. (2013). Ocean currents structuring the mesozooplankton in the Gulf of Mannar and the Palk Bay, southeast coast of India. *Progress in Oceanography*, 110, 27-48.

James, A., Hu, J., Emile-Geay, J., Partin, J. W., Scroxton, N., Malik, N., & Gao, Y. (2025). Regime shifts in Holocene paleohydrology as recorded by Asian speleothems. *Paleoceanography and Paleoclimatology*, 40, e2024PA004974.

Jayalakshmi, K. J., Sabu, P., Devi, C. A., & Sanjeevan, V. N. (2015). Response of micro-and mesozooplankton in the southwestern Bay of Bengal to a cyclonic eddy during the winter monsoon, 2005. *Environmental monitoring and assessment*, 187, 1-18.

Kathayat, G., Cheng, H., Sinha, A., Yi, L., Li, X., Zhang, H., Li, H., Ning, Y. and Edwards, R.L. (2017). The Indian monsoon variability and civilization changes in the Indian subcontinent. *Science advances*, 3 (12), e1701296.

Katz, ME., Cramer, BS., Franzese, A., Honisch, B., Miller, KG., Rosenthal, Y., Wright, J. D. (2010). Traditional and emerging geochemical proxies in Foraminifera. *The Journal of Foraminiferal Research*, 40 (2), 165–192.

Kessarkar PM and Rao VP (2007) Organic carbon in sediments of the southwestern margin of India: influence of productivity and monsoon variability during the Late Quaternary. *Journal of the Geological Society of India*, 69, 42–52.

Khan, I., Sinha, R., Murray, A. S., & Jain, M. (2024). Landscape evolution of the NW Himalayan rivers during the late Quaternary and their non-contemporaneity to the Harappan Civilization. *Quaternary Science Reviews*, 331, 108622.

Khole, M., & De, U. S. (2003). A study on north-east monsoon rainfall over India. *Mausam*, 54 (2), 419-426.

Kripalani, R. H., & Kumar, P. (2004). Northeast monsoon rainfall variability over south peninsular India vis-à-vis the Indian Ocean dipole mode. *International Journal of Climatology: A Journal of the Royal Meteorological Society*, 24 (10), 1267-1282.

Krishna Kumar, K., Rupa Kumar, K., Ashrit, R. G., Deshpande, N. R., & Hansen, J. W. (2004). Climate impacts on Indian agriculture. *International Journal of Climatology: A Journal of the Royal Meteorological Society*, 24 (11), 1375-1393.

Krishnamurthy, V., & Shukla, J. (2000). Intraseasonal and interannual variability of rainfall over India. *Journal of climate*, 13 (24), 4366-4377.

Kucera, M. (2007). Planktonic foraminifera as tracers of past oceanic environments, Chapter 6. *Developments in Marine Geology*, *Elsevier*, 1, 213-262.

Kudrass, H. R., Hofmann, A., Doose, H., Emeis, K., & Erlenkeuser, H. (2001). Modulation and amplification of climatic changes in the Northern Hemisphere by the Indian summer monsoon during the past 80 ky. *Geology*, 29 (1), 63-66.

Kumar, S. P., Narvekar, J., Nuncio, M., Kumar, A., Ramaiah, N., Sardesai, S., Gauns, M., Fernandes, V. and Paul, J. (2010). Is the biological productivity in the Bay of Bengal light limited?. *Current science*, 1331-1339.

Lamb, A. L., Wilson, G. P., & Leng, M. J. (2006). A review of coastal palaeoclimate and relative sea-level reconstructions using δ13C and C/N ratios in organic material. *Earth-Science Reviews*, *75*(1-4), 29-57.

Laskar, A. H., & Bohra, A. (2021). Impact of Indian summer monsoon change on ancient Indian civilizations during the Holocene. *Frontiers in Earth Science*, 9, 709455.

Latif, M., & Keenlyside, N. S. (2009). El Niño/Southern Oscillation response to global warming. *Proceedings of the National Academy of Sciences*, 106 (49), 20578-20583.

Li, Y., Song, Y., Yin, Q., Han, L., & Wang, Y. (2019). Orbital and millennial northern mid-latitude westerlies over the last glacial period. *Climate Dynamics*, 53 (5), 3315-3324.

https://doi.org/10.5194/egusphere-2026-4747
Preprint. Discussion started: 1 September 2026


Liu, S., Ye, W., Cao, P., Zhang, H., Chen, M.T., Li, X., Li, J., Pan, H.J., Khokiattiwong, S., Kornkanitnan, N. and Shi, X. (2021). Paleoclimatic responses in the tropical Indian Ocean to regional monsoon and global climate change over the last 42 kyr. *Marine Geology*, 438, 106542.

Liu, W., Fedorov, A. V., Xie, S. P., & Hu, S. (2020). Climate impacts of a weakened Atlantic Meridional Overturning Circulation in a warming climate. *Science advances*, 6 (26), eaaz4876.

Locarnini RA, Mishonov AV, Baranova OK, Boyer TP, Zweng MM, Garcia HE, Reagan JR, Seidov D, Weathers K, Paver CR, Smolyar IV (2019) World Ocean Atlas 2018, Volume 1: temperature. Mishonov Technical A (Ed), NOAA Atlas NESDIS 81:52

Loveson, V. J., & Nigam, R. (2019). Reconstruction of Late Pleistocene and Holocene sea level curve for the east coast of India. *Journal of the Geological Society of India*, 93, 507-514.

Lu, R., Dong, B., & Ding, H. (2006). Impact of the Atlantic Multidecadal Oscillation on the Asian summer monsoon. *Geophysical Research Letters*, 33 (24).

Madhupratap, M., Gauns, M., Ramaiah, N., Kumar, S.P., Muraleedharan, P.M., De Sousa, S.N., Sardessai, S. and Muraleedharan, U., (2003). Biogeochemistry of the Bay of Bengal: physical, chemical and primary productivity characteristics of the central and western Bay of Bengal during summer monsoon 2001. *Deep Sea Research Part II: Topical Studies in Oceanography*, 50, 881-896.

Maeda, A., Kuroyanagi, A., Iguchi, A., Gaye, B., Rixen, T., Nishi, H., & Kawahata, H. (2022). Seasonal variation of fluxes of planktic foraminiferal tests collected by a time-series sediment trap in the central Bay of Bengal during three different years. *Deep Sea Research Part I: Oceanographic Research Papers*, 183, 103718.

Mayewski, P. A., Rohling, E. E., Stager, J. C., Karlén, W., Maasch, K. A., Meeker, L. D., Meyerson, E. A., Gasse, F., van Kreveld, S., Holmgren, K., Lee-Thorp, J., Rosqvist, G., Rack, F., Staubwasser, M., Schneider, R. R., & Steig, E. J. (2004). Holocene climate variability. *Quaternary research*, 62 (3), 243-255.

Mazumder, A., Khare, N., & Govil, P. (2009). Cosmopolitanism of the planktic foraminiferal species Globigerinita glutinata–A testimony by Q-mode cluster analysis. *International Journal of Geology*, 1 (3), 1-7.

McKay, N.P., Kaufman, D.S., Arcusa, S.H., Kolus, H.R., Edge, D.C., Erb, M.P., Hancock, C.L., Routson, C.C., Zarczynski, M., Marshall, L.P., & Roberts, G.K. (2024). The 4.2 ka event is not remarkable in the context of Holocene climate variability. *Nature Communications*, 15, 6555.

Meyers, P. A. (1994). Preservation of elemental and isotopic source identification of sedimentary organic matter. *Chemical geology*, *114*(3-4), 289-302.

Moy, C. M., Seltzer, G. O., Rodbell, D. T., & Anderson, D. M. (2002). Variability of El Niño/Southern Oscillation activity at millennial timescales during the Holocene epoch. *Nature*, 420, 162-165.

Muraleedharan, K. R., Jasmine, P., Achuthankutty, C. T., Revichandran, C., Kumar, P. D., Anand, P., & Rejomon, G. (2007). Influence of basin-scale and mesoscale physical processes on biological productivity in the Bay of Bengal during the summer monsoon. *Progress in Oceanography*, 72 (4), 364-383.

Naidu, P. D., Ganeshram, R., Bollasina, M. A., Panmei, C., Nürnberg, D., & Donges, J. F. (2020). Coherent response of the Indian Monsoon Rainfall to Atlantic Multi-decadal Variability over the last 2000 years. *Scientific Reports*, 10 (1), 1302.

Naidu, P. D., Ramesh Kumar, M. R., & Ramesh Babu, V. (1999). Time and space variations on monsoonal upwelling along the west and east coasts of India. *Continental shelf research*, 19 (4), 559-572.

Nan, Q., Chen, S., Liu, X., Ma, S., Sun, Y., Huang, L., Chen, J., Luterbacher, J., Meadows, M.E., & Chen, F. (2025). The 4.2 ka event in the Northern Hemisphere: Spatial heterogeneity and driving mechanisms of hydroclimatic change. *Earth-Science Reviews*, 265, 105128.

https://doi.org/10.5194/egusphere-2026-4747
Preprint. Discussion started: 1 September 2026


Nigam R (2005) Addressing environmental issues through foraminifera–case studies from the Arabian Sea. *Journal of the Palaeontological Society of India*, 50 (2), 25-36.

Olsen, J., Anderson, N. J., & Knudsen, M. F. (2012). Variability of the North Atlantic Oscillation over the past 5,200 years. *Nature Geoscience*, 5 (11), 808-812.

Ovechkina, M. N., Bylinskaya, M. E., & Uken, R. (2010). Planktonic foraminiferal assemblage in surface sediments from the Thukela Shelf, South Africa. *African Invertebrates*, 51 (2), 231-254. https://hdl.handle.net/10520/EJC84679

Parker, F. L. (1962). Planktonic foraminiferal species in Pacific sediments. *micropaleontology*, 8 (2), 219-254.

Peketi, A., Mazumdar, A., Pillutla, S. P. K., Rai, V. K., Sawant, B., & Chaitanya, A. V. S. (2020). Monsoon rainfall and contrasting source rocks influenced sediment composition of peninsular basins along the east coast of India (western Bay of Bengal). *Marine and Petroleum Geology*, 118, 104433.

Phillips, S. C., Johnson, J. E., Giosan, L., & Rose, K. (2014). Monsoon-influenced variation in productivity and lithogenic sediment flux since 110 ka in the offshore Mahanadi Basin, northern Bay of Bengal. *Marine and Petroleum Geology*, 58, 502-525.

Ponton, C., Giosan, L., Eglinton, T. I., Fuller, D. Q., Johnson, J. E., Kumar, P., & Collett, T. S. (2012). Holocene aridification of India. *Geophysical Research Letters*, 39 (3).

Prasad, S., Anoop, A., Riedel, N., Sarkar, S., Menzel, P., Basavaiah, N., Krishnan, R., Fuller, D., Plessen, B., Gaye, B. and Röhl, U. (2014). Prolonged monsoon droughts and links to Indo-Pacific warm pool: A Holocene record from Lonar Lake, central India. *Earth and Planetary Science Letters*, 391, 171-182.

Prasanna Kumar, S., Muraleedharan, P. M., Prasad, T. G., Gauns, M., Ramaiah, N., De Souza, S. N., Sardesai, S. & Madhupratap, M. (2002). Why is the Bay of Bengal less productive during summer monsoon compared to the Arabian Sea?. *Geophysical research letters*, 29 (24), 88-1.

Prasanna Kumar, S., Nuncio, M., Narvekar, J., Kumar, A., Sardesai, D. S., De Souza, S. N., Gauns, M., Ramaiah, N. and Madhupratap, M. (2004). Are eddies nature's trigger to enhance biological productivity in the Bay of Bengal?. *Geophysical Research Letters*, 31 (7).

Prasanna, V. (2014). Impact of monsoon rainfall on the total foodgrain yield over India. *Journal of earth system science*, 123 (5), 1129-1145.

Psomiadis, D., Dotsika, E., Albanakis, K., Ghaleb, B., & Hillaire-Marcel, C. (2018). Speleothem record of climatic changes in the northern Aegean region (Greece) from the Bronze Age to the collapse of the Roman Empire. *Palaeogeography, Palaeoclimatology, Palaeoecology*, 489, 272-283.

Railsback, L.B., Liang, F., Brook, G.A., Voarintsoa, N.R.G., Sletten, H.R., Marais, E., Hardt, B., Cheng, H. and Edwards, R.L. (2018). The timing, two-pulsed nature, and variable climatic expression of the 4.2 ka event: A review and new high-resolution stalagmite data from Namibia. *Quaternary Science Reviews*, 186, 78-90.

Ran, M., & Chen, L. (2019). The 4.2 ka BP climatic event and its cultural responses. *Quaternary international*, *521*, 158-167.

Rashid, H., England, E., Thompson, L., & Polyak, L. (2011). Late glacial to Holocene Indian summer monsoon variability based upon sediment records taken from the Bay of Bengal. *TAO: Terrestrial, Atmospheric and Oceanic Sciences*, 22 (2), 2.

Ratna, S. B., Sabeerali, C. T., Sharma, T., Pai, D. S., & Mohapatra, M. (2024). Combined influence of El Niño, IOD and MJO on the Indian Summer Monsoon Rainfall: Case Study for the years 1997 and 2015. *Atmospheric Research*, 299, 107214.

Ravelo, A. C., & Fairbanks, R. G. (1992). Oxygen isotopic composition of multiple species of planktonic foraminifera: recorders of the modern photic zone temperature gradient. *Paleoceanography,* 7 (6), 815-831.

https://doi.org/10.5194/egusphere-2026-4747
Preprint. Discussion started: 1 September 2026


Ravelo, A. C., Fairbanks, R. G., & Philander, S. G. H. (1990). Reconstructing tropical Atlantic hydrography using planktontic foraminifera and an ocean model. *Paleoceanography*, 5 (3), 409-431.

Reynolds, L., & Thunell, R. C. (1985). Seasonal succession of planktonic foraminifera in the subpolar North Pacific. *The Journal of Foraminiferal Research*, 15 (4), 282-301.

Saalim, S. M., Saraswat, R., & Nigam, R. (2022). Ecological preferences of living benthic foraminifera from the Mahanadi river-dominated north-western Bay of Bengal: A potential environmental impact assessment tool. *Marine Pollution Bulletin*, 175, 113158.

Sabu, P., Devi, C. A., Lathika, C. T., Sanjeevan, V. N., & Gupta, G. V. M. (2015). Characteristics of a cyclonic eddy and its influence on mesozooplankton community in the northern Bay of Bengal during early winter monsoon. *Environmental monitoring and assessment*, 187, 1-19.

Saji, N. H., Goswami, B. N., Vinayachandran, P. N., & Yamagata, T. (1999). A dipole mode in the tropical Indian Ocean. *Nature*, 401 (6751), 360-363.

Salman, M., & Saraswat, R. (2024). Intrusion of Arabian Sea high salinity water and monsoon-associated processes modulate planktic foraminiferal abundance and carbon burial in the southwestern Bay of Bengal. *Environmental Science and Pollution Research*, 31 (17), 24961-24985.

Sandeep, K. K., & Pant, V. (2019). Riverine freshwater plume variability in the Bay of Bengal using wind sensitivity experiments. *Deep Sea Research Part II: Topical Studies in Oceanography*, 168, 104649.

Sandeep, K., Shankar, R., Warrier, A.K., Yadava, M.G., Ramesh, R., Jani, R.A., Weijian, Z. and Xuefeng, L. (2017). A multi-proxy lake sediment record of Indian summer monsoon variability during the Holocene in southern India. *Palaeogeography, palaeoclimatology, palaeoecology*, 476, 1-14.

Saraswat, R. (2015). Non-destructive foraminiferal paleoclimatic proxies: A brief insight, *Proceedings of the Indian National Science Academy*, 81(2).

Saraswat, R., Naik, D. K., Nigam, R., & Gaur, A. S. (2016). Timing, cause and consequences of mid-Holocene climate transition in the Arabian Sea. *Quaternary Research*, 86 (2), 162-169.

Saraswat, R., Rajput, K.R., Bandodkar, S.R., Bhadra, S.R., Kurtarkar, S.R., Joäo, H.M., Suokhrie, T. & Kumar, P. (2023a). Persistent increase in carbon burial in the Gulf of Mannar, during the Meghalayan Age: Influence of primary productivity and better preservation. *Geological Magazine*, 160 (3), 561-578.

Saraswat, R., Suokhrie, T., Naik, D. K., Singh, D. P., Saalim, S. M., Salman, M., Kumar, G., Bhadra, S. R., Mohtadi, M., Kurtarkar, S. R., & Maurya, A. S. (2023b). Large freshwater-influx-induced salinity gradient and diagenetic changes in the northern Indian Ocean dominate the stable oxygen isotopic variation in Globigerinoides ruber. *Earth System Science Data*, 15 (1), 171-187.

Saravanan, P., Gupta, A. K., Zheng, H., Panigrahi, M. K., & Prakasam, M. (2019). Late Holocene long arid phase in the Indian subcontinent as seen in shallow sediments of the eastern Arabian Sea. *Journal of Asian Earth Sciences*, *181*, 103915.

Sarma, V. V. S. S., Rao, G. D., Viswanadham, R., Sherin, C. K., Salisbury, J., Omand, M. M., Mahadevan, A., Murty, V. S. N., Shroyer, E.L., Baumgartner, M. and Stafford, K. M. (2016). Effects of freshwater stratification on nutrients, dissolved oxygen, and phytoplankton in the Bay of Bengal. *Oceanography*, 29 (2), 222-231.

Schiebel, R., & Hemleben, C. (2000). Interannual variability of planktic foraminiferal populations and test flux in the eastern North Atlantic Ocean (JGOFS). *Deep Sea Research Part II: Topical Studies in Oceanography*, 47 (9-11), 1809-1852.

Schiebel, R., & Hemleben, C. (2017). Planktic foraminifers in the modern ocean. *Springer Berlin, Heidelberg*, 358, 978-3.

Schiebel, R., Waniek, J., Bork, M., & Hemleben, C. (2001). Planktic foraminiferal production stimulated by chlorophyll redistribution and entrainment of nutrients. *Deep Sea Research Part I: Oceanographic Research Papers*, *48*(3), 721-740.

https://doi.org/10.5194/egusphere-2026-4747
Preprint. Discussion started: 1 September 2026



Schmuker, B., & Schiebel, R. (2002). Planktic foraminifers and hydrography of the eastern and northern Caribbean Sea. *Marine Micropaleontology*, 46 (3-4), 387-403.

Schneider, T., Bischoff, T., & Haug, G. H. (2014). Migrations and dynamics of the intertropical convergence zone. *Nature*, 513 (7516), 45-53.

Schott, F. A., & McCreary Jr, J. P. (2001). The monsoon circulation of the Indian Ocean. *Progress in Oceanography*, 51 (1), 1-123.

Schulz, H., Von Rad, U., & Ittekkot, V. (2002). Planktic foraminifera, particle flux and oceanic productivity off Pakistan, NE Arabian Sea: modern analogues and application to the palaeoclimatic record. *Geological Society, London, Special Publications*, 195 (1), 499-516.

Sejrup, H. P., Haflidason, H., & Andrews, J. T. (2011). A Holocene North Atlantic SST record and regional climate variability. *Quaternary Science Reviews*, 30 (21-22), 3181-3195.

Sengupta, T., Deshpande Mukherjee, A., Bhushan, R., Ram, F., Bera, M.K., Raj, H., Dabhi, A.J., Bisht, R.S., Rawat, Y.S., Bhattacharya, S.K. & Juyal, N. (2020). Did the Harappan settlement of Dholavira (India) collapse during the onset of Meghalayan stage drought?. *Journal of Quaternary Science*, 35 (3), 382-395.

Shankar, D., Vinayachandran, P. N., & Unnikrishnan, A. S. (2002). The monsoon currents in the north Indian Ocean. *Progress in oceanography*, 52 (1), 63-120.

Sharifi, A., Pourmand, A., Canuel, E. A., Ferer-Tyler, E., Peterson, L. C., Aichner, B., Feakins, S. J., Daryaee, T., Djamali, M., Beni, A. N., Lahijani, H. A. K., & Swart, P. K. (2015). Abrupt climate variability since the last deglaciation based on a high-resolution, multi-proxy peat record from NW Iran: The hand that rocked the cradle of civilization? *Quaternary Science Reviews*, 123, 215–230.

Shetye, S. R., Shenoi, S. S. C., Gouveia, A. D., Michael, G. S., Sundar, D., & Nampoothiri, G. (1991). Wind-driven coastal upwelling along the western boundary of the Bay of Bengal during the southwest monsoon. *Continental Shelf Research*, 11 (11), 1397-1408.

Shrivastav, A., Singh, A. K., Sinha, D. K., Kaushik, T., Singh, V. P., & Mallick, K. (2016). Significance of Globigerina bulloides d'orbigny: A foraminiferal proxy for palaeomonsoon and past upwelling records. *Journal of climate change*, 2 (2), 99-110.

Sijinkumar, A. V., Clemens, S., Nath, B. N., Prell, W., Benshila, R., & Lengaigne, M. (2016). δ18O and salinity variability from the Last Glacial Maximum to Recent in the Bay of Bengal and Andaman Sea. *Quaternary Science Reviews*, 135, 79-91.

Singh, A. D., Jung, S. J. A., Darling, K., Ganeshram, R., Ivanochko, T., & Kroon, D. (2011). Productivity collapses in the Arabian Sea during glacial cold phases. *Paleoceanography*, 26, PA3210.

Singh, A. D., Jung, S. J., Darling, K., Ganeshram, R., Ivanochko, T., & Kroon, D. (2011). Productivity collapses in the Arabian Sea during glacial cold phases. *Paleoceanography*, 26, PA3210.

Singh, P., & Rajamani, V. (2001). Geochemistry of the floodplain sediments of the Kaveri River, southern India. *Journal of sedimentary Research*, 71 (1), 50-60.

Stanley, J. D., Krom, M. D., Cliff, R. A., & Woodward, J. C. (2003). Short contribution: Nile flow failure at the end of the Old Kingdom, Egypt: strontium isotopic and petrologic evidence. *Geoarchaeology*, 18 (3), 395-402.

Staubwasser, M., Sirocko, F., Grootes, P. M., & Segl, M. (2003). Climate change at the 4.2 ka BP termination of the Indus valley civilization and Holocene south Asian monsoon variability. *Geophysical Research Letters*, 30 (8).

Stoll, H. M., Arevalos, A., Burke, A., Ziveri, P., Mortyn, G., Shimizu, N., & Unger, D. (2007). Seasonal cycles in biogenic production and export in Northern Bay of Bengal sediment traps. *Deep Sea Research Part II: Topical Studies in Oceanography*, 54 (5-7), 558-580.

Stouffer, R. J., Yin, J. J., Gregory, J., Dixon, K., Spelman, M., Hurlin, W., Weaver, A., Eby, M., Flato, G., Hasumi, H., Hu, A., Jungclaus, J., Kamenkovich, I., Levermann, A., Montoya, M., Murakami, S., Nawrath, S., Oka, A., Peltier, W., Robitaille, D., Sokolov, A., Vettoretti, G., & Weber, S. (2006).

https://doi.org/10.5194/egusphere-2026-4747
Preprint. Discussion started: 1 September 2026


Investigating the causes of the response of the thermohaline circulation to past and future climate changes. *Journal of climate*, 19 (8), 1365-1387.

Subramanian, V. (1978). Input by Indian rivers into the world oceans. *Proceedings of the Indian Academy of Sciences-Section A, Earth and Planetary Sciences*, 87, 77-88.

Sun, L., Shen, B., Sui, B., & Huang, B. (2017). The influences of East Asian Monsoon on summer precipitation in Northeast China. *Climate Dynamics*, 48 (5), 1647-1659.

Suokhrie, T., & Saraswat, R. (2024). Large shift in the upper water column characteristics of the west-central Bay of Bengal during the last glacial-interglacial transition. *Palaeogeography, Palaeoclimatology, Palaeoecology*, 635, 111957.

Suokhrie, T., Saraswat, R., & Saju, S. (2021). Strong solar influence on multi-decadal periodic productivity changes in the central-western Bay of Bengal. *Quaternary International*, 629, 16-26.

Thamban, M., Kawahata, H., & Rao, V. P. (2007). Indian summer monsoon variability during the Holocene as recorded in sediments of the Arabian Sea: timing and implications. *Journal of oceanography*, 63, 1009-1020.

Toledo, F. A., Costa, K. B., Pivel, M. A., & Campos, E. J. (2008). Tracing past circulation changes in the western South Atlantic based on planktonic foraminifera. *Revista Brasileira de Paleontologia*, 11 (3), 169-178.

Toth, L. T., & Aronson, R. B. (2019). The 4.2 ka event, ENSO, and coral reef development. *Climate of the Past*, 15 (1), 105-119.

Trask, P. D. (1938). Relation of salinity to the calcium carbonate content of marine sediments. 186, 273–299.

Vaithiyanathan, P., Ramanathan, A. L., & Subramanian, V. (1988). Erosion, transport and deposition of sediments by the tropical rivers of India. *IN: Sediment Budgets. IAHS Publication*, 174, 561-574.

Verma, K., Singh, A. D., Singh, P., Singh, H., Satpathy, R. K., Uddandam, P. R., & Naidu, P. D. (2022). Monsoon-related changes in surface hydrography and productivity in the Bay of Bengal over the last 45 kyr BP. *Palaeogeography, Palaeoclimatology, Palaeoecology*, 589, 110844.

Vinayachandran, P. N., Masumoto, Y., Mikawa, T., & Yamagata, T. (1999). Intrusion of the southwest monsoon current into the Bay of Bengal. *Journal of Geophysical Research: Oceans*, 104 (C5), 11077-11085.

Vinayachandran, P. N., McCreary Jr, J. P., Hood, R. R., & Kohler, K. E. (2005). A numerical investigation of the phytoplankton bloom in the Bay of Bengal during Northeast Monsoon. *Journal of Geophysical Research: Oceans*, 110 (C12).

Vinayachandran, P. N., Murty, V. S. N., & Ramesh Babu, V. (2002). Observations of barrier layer formation in the Bay of Bengal during summer monsoon. *Journal of Geophysical Research: Oceans*, 107 (C12), SRF-19.

Vinayachandran, P. N., Shankar, D., Vernekar, S., Sandeep, K. K., Amol, P., Neema, C. P., & Chatterjee, A. (2013). A summer monsoon pump to keep the Bay of Bengal salty. *Geophysical Research Letters*, 40 (9), 1777-1782.

Vybhav, K., Narasimha, K. N. P., Nagendra, R., Mujumdar, P. P., & krishnan, N. G. (2020). Geochemical appraisal of sediments from River Cauvery, Tamilnadu: an insight into its sediment maturity, provenance, and tectonic setting. *Journal of Engineering Sciences*, 11, 101-110.

Walker, M., Gibbard, P., Head, M.J., Berkelhammer, M., Björck, S., Cheng, H., Cwynar, L.C., Fisher, D., Gkinis, V., Long, A. and Lowe, J. (2019). Formal subdivision of the Holocene Series/Epoch: A summary. *Journal of the Geological Society of India*, 93, 135-141.

Wang, Y., Cheng, H., Edwards, R. L., He, Y., Kong, X., An, Z., Wu, J., Kelly, M. J., Dykoski, C. A., & Li, X. (2005). The holocene asian monsoon: Links to solar changes and North Atlantic Climate. *Science*, 308 (5723), 854-857.

https://doi.org/10.5194/egusphere-2026-4747
Preprint. Discussion started: 1 September 2026


Wu, Y.J., Ji, H.X., Wen, J.H., Wu, S.Y., Xu, M., Tagle, F., He, B., Duan, W.L., & Li, J.X. (2019). The characteristics of regional heavy precipitation events over eastern monsoon China during 1960-2013. *Global and Planetary Change*, 172, 414-427.

Yadav, R., Naik, S. S., & Narvekar, J. (2022). The equatorial Indian Ocean upper water-column structure influenced by cross-basinal water exchange over the last~ 40000 years. *Quaternary International*, *642*, 84-92.

Zarkogiannis, S.D., Iwasaki, S., Rae, J.W.B., Schmidt, M.W., Mortyn, P.G., Kontakiotis, G., Hertzberg, J.E. and Rickaby, R.E. (2022). Calcification, dissolution and test properties of modern planktonic foraminifera from the central Atlantic Ocean. *Frontiers in Marine Science*, 9, 864801.

Zhang, R., & Delworth, T. L. (2005). Simulated tropical response to a substantial weakening of the Atlantic thermohaline circulation. *Journal of climate*, 18 (12), 1853-1860.

Zhao, J., An, C. B., Huang, Y., Morrill, C., & Chen, F. H. (2017). Contrasting early Holocene temperature variations between monsoonal East Asia and westerly dominated Central Asia. *Quaternary Science Reviews*, *178*, 14-23.Zweng MM, Reagan JR, Seidov D, Boyer TP, Locarnini RA, Garcia HE, Mishonov AV, Baranova OK, Weathers K, Paver CR, Smolyar IV (2019) World Ocean Atlas 2018, Volume 2: Salinity. Mishonov Technical A (Ed), NOAA Atlas NESDIS 82:50.

https://doi.org/10.5194/egusphere-2026-4747
Preprint. Discussion started: 1 September 2026


## Legend to Figures and Tables

**Figure 1.** The core location (SSD067 PC03) in the southwestern Bay of Bengal is marked by red dot. The small black arrows are the wind pattern during July month and the bigger orange and blue arrows represent the summer and winter monsoon patterns, respectively. The light orange and white arrows represent surface ocean currents during the summer and winter season along the east and west coast of India. The background is the annual average salinity. The blue lines mark the major rivers. The bar and line graph (b) shows the monthly mean rainfall in Tamil Nadu state and freshwater discharge of Cauvery River, and the wind rose diagram (c) shows the seasonally dominant wind pattern at the core location.

**Figure 2.** Seasonal changes in temperature, salinity, and chlorophyll-a in the southwestern Bay of Bengal. The black dot is the core location (SSD067 PC03). The blue lines mark the major rivers.

**Figure 3.** Age-depth profile and sedimentation rate in the studied section of core SSD067 PC03. The green colour dots represent dated intervals with black solid line, which is the median age-depth profile. The purple dotted lines represent the minimum and maximum age range with a 95% confidence level (2σ age uncertainty). The solid orange line represents the depth profile of sedimentation rate. The 4.2 ka event is marked by the light blue-green bar.

**Figure 4.** The variation in coarse fraction (CF), total carbon (TC), organic carbon ($C_{org}$), total inorganic carbon (TIC), and nitrogen (N) percentage during the 4.2 ka event in the southwestern Bay of Bengal. Phases of the 4.2 ka event are marked by the faded pink colour and light blue-green bars, respectively.

**Figure 5.** Scatter plots showing the relationship between coarse fraction (CF), total planktic foraminifera number (TPN), Calcium carbonate ($CaCO_3$), and organic carbon ($C_{org}$) in sediment core (SSD067 PC03) collected from the southwestern Bay of Bengal. (a) CF vs. TPN, (b) CF vs. $CaCO_3$, (c) TPN vs. $CaCO_3$, and (d) $CaCO_3$ vs. $C_{org}$. The solid lines represent linear regression fits. The coefficient of

https://doi.org/10.5194/egusphere-2026-4747
Preprint. Discussion started: 1 September 2026


determination ($R^2$) significance level (p) and sample size (n) are indicated in each panel. TPN data are available for alternate depth intervals (n = 51) while CF, CaCO3, and $C_{org}$ were measured at all sampled depths (n = 101).

**Figure 6.** Variation in relative abundance of planktic foraminiferal species during the 4.2 ka event in the southwestern Bay of Bengal. The solid lines represent a 3-point moving average for six dominant species with an average relative abundance >5%. Phases of the 4.2 ka event are marked by the faded pink colour and light blue-green bars, respectively.

**Figure 7.** The variation in $CaCO_3$, $C_{org}$, $C_{org}$/N, *G. bulloides*/*G. ruber*, summer and winter monsoon assemblages (SMA and WMA) during the 4.2 ka event in the southwestern Bay of Bengal. Phases of the 4.2 ka event are marked by the faded pink colour and light blue-green bars, respectively.

**Figure 8.** Comparison of $CaCO_3$ and $C_{org}$ in SSD067 PC03 with other marine records from the North Indian Ocean [SSD004 GC02 (Saraswat et al., 2023); SK308 GC02 (Suokhrie et al., 2021)], and terrestrial records from India [Kotla Dahar Lake (Dixit et al., 2014b); Lonar Lake (Prasad et al., 2014)]. The marine and terrestrial records of the monsoon variability during the 4.2 ka event [SSD067 PC03 (This study); SSD004 GC02 (Saraswat et al., 2023a); SK308 GC02 (Suokhrie and Saraswat, 2024); SO93-126KL (Kudrass et al., 2001); NGHP-01-16A (Ponton et al., 2012); SK291 GC15 (Saravanan et al., 2021); SO90-63KA (Burdanowitz et al., 2020); terrestrial record from India, Kotla Dahar Lake (Dixit et al., 2014); and a speleothem records from northeast India, KM-A (Berkelhammer et al., 2012)].

**Figure 9.** The changes in summer and winter monsoon (SMA and WMA), carbon burial, modelled AMOC strength (Gerber et al., 2024), Z-score of sortable silt (10-63 µm) based reconstructed AMOC strength (Hoogakker et al., 2011), ENSO activity (Moy et al., 2002), global sea level (Grant et a., 2014), and western Bay of Bengal sea level (Loveson and Nigam, 2019) during the 4.2 ka event.

https://doi.org/10.5194/egusphere-2026-4747
Preprint. Discussion started: 1 September 2026


**Table 1:** Details of the radiocarbon dates with lab code, associated errors, 2 sigma age range, calibrated median ages, and sedimentation rate.

**Table 2:** Mean values of sediment geochemical and foraminiferal proxies during the pre-event (before 4.65 ka), event (4.65-3.97 ka), and post event (after 3.97 ka) intervals of the 4.2 ka event recorded in sediment core (SSD067 PC03) from the southwestern Bay of Bengal. The event interval is subdivided into two phases, namely Phase 1(4.65-4.45 ka) and Phase 2 (4.45-3.97 ka).

https://doi.org/10.5194/egusphere-2026-4747
Preprint. Discussion started: 1 September 2026


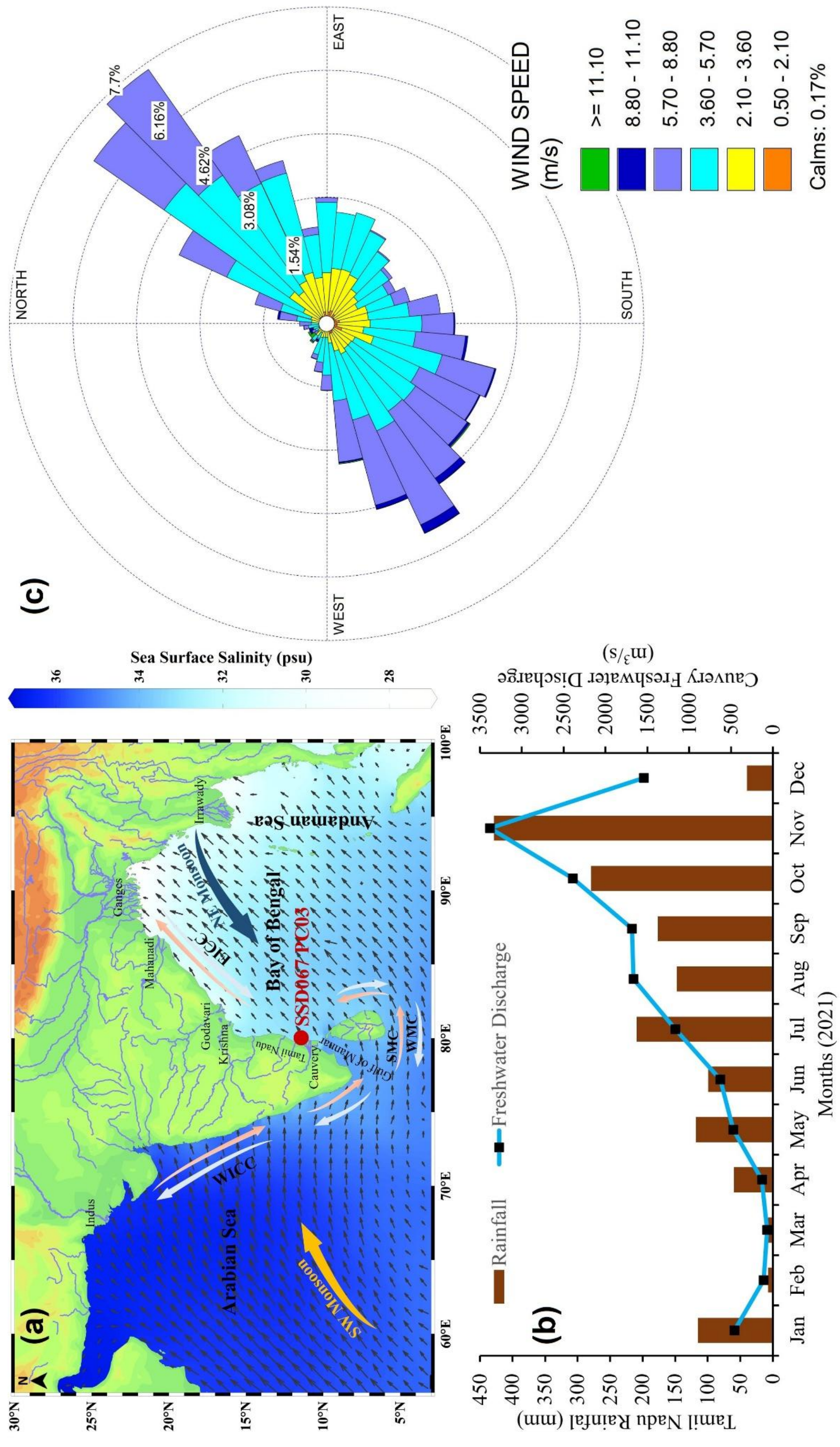


**Figure 1**

https://doi.org/10.5194/egusphere-2026-4747
Preprint. Discussion started: 1 September 2026


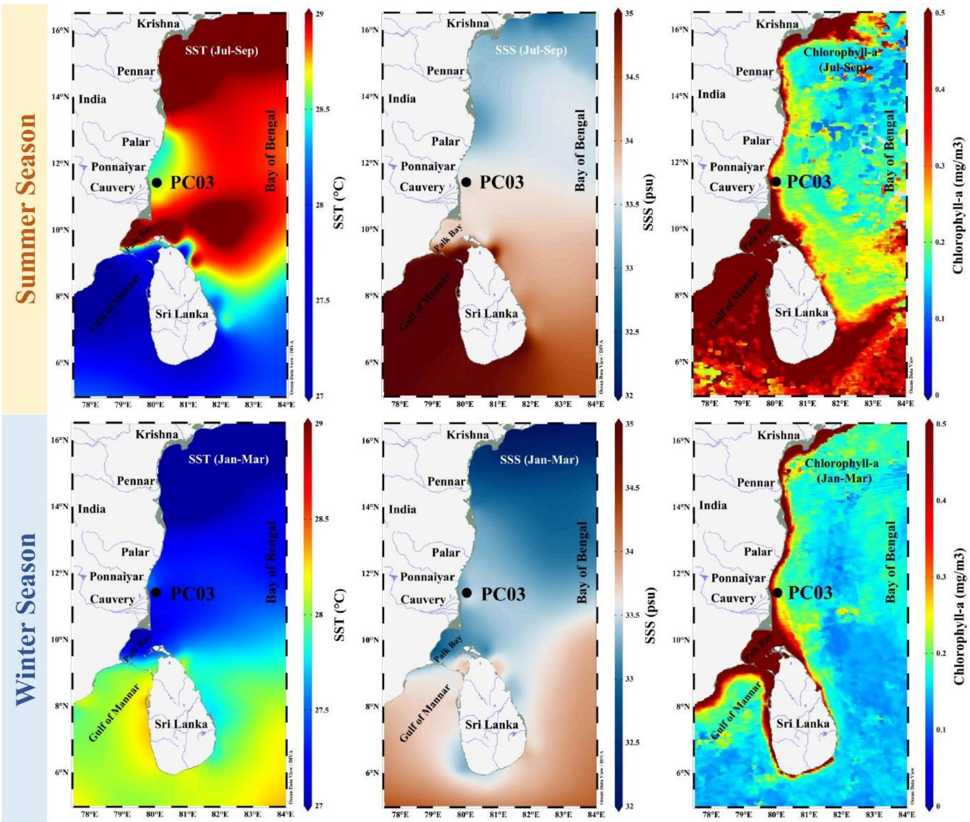


**Figure 2**

https://doi.org/10.5194/egusphere-2026-4747
Preprint. Discussion started: 1 September 2026


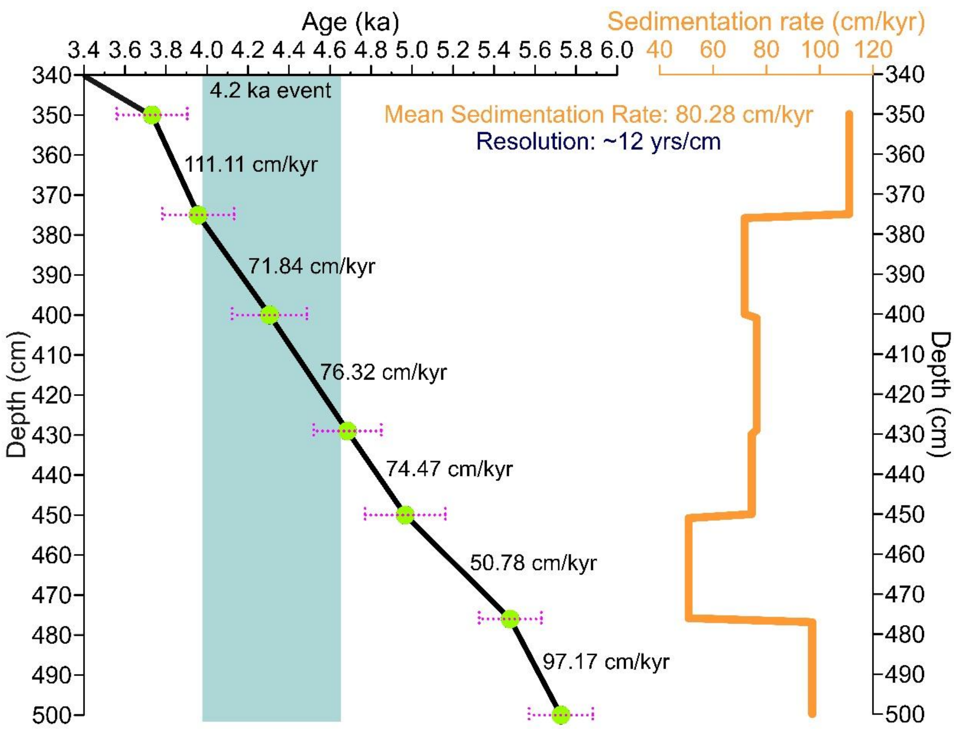


**Figure** 3

https://doi.org/10.5194/egusphere-2026-4747
Preprint. Discussion started: 1 September 2026




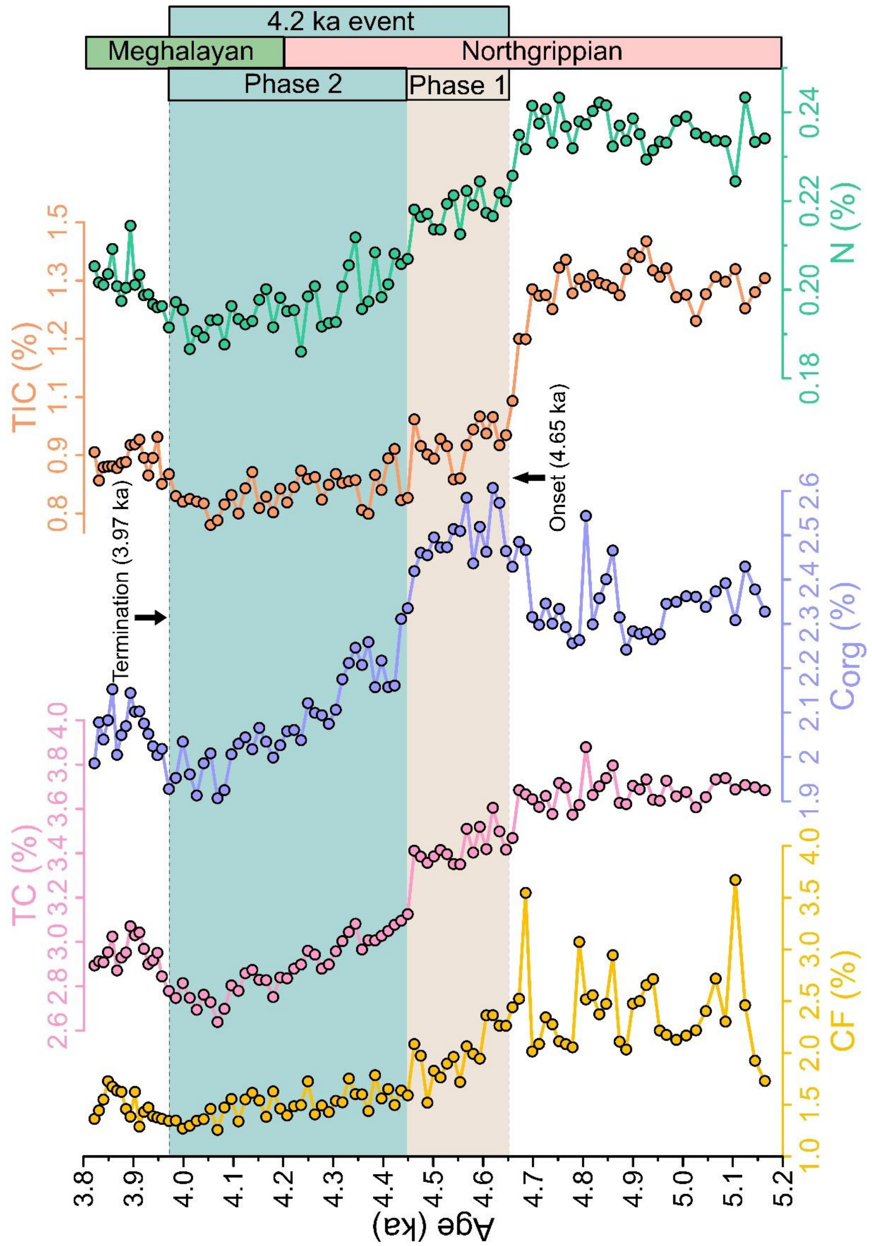


**Figure 4**

https://doi.org/10.5194/egusphere-2026-4747
Preprint. Discussion started: 1 September 2026


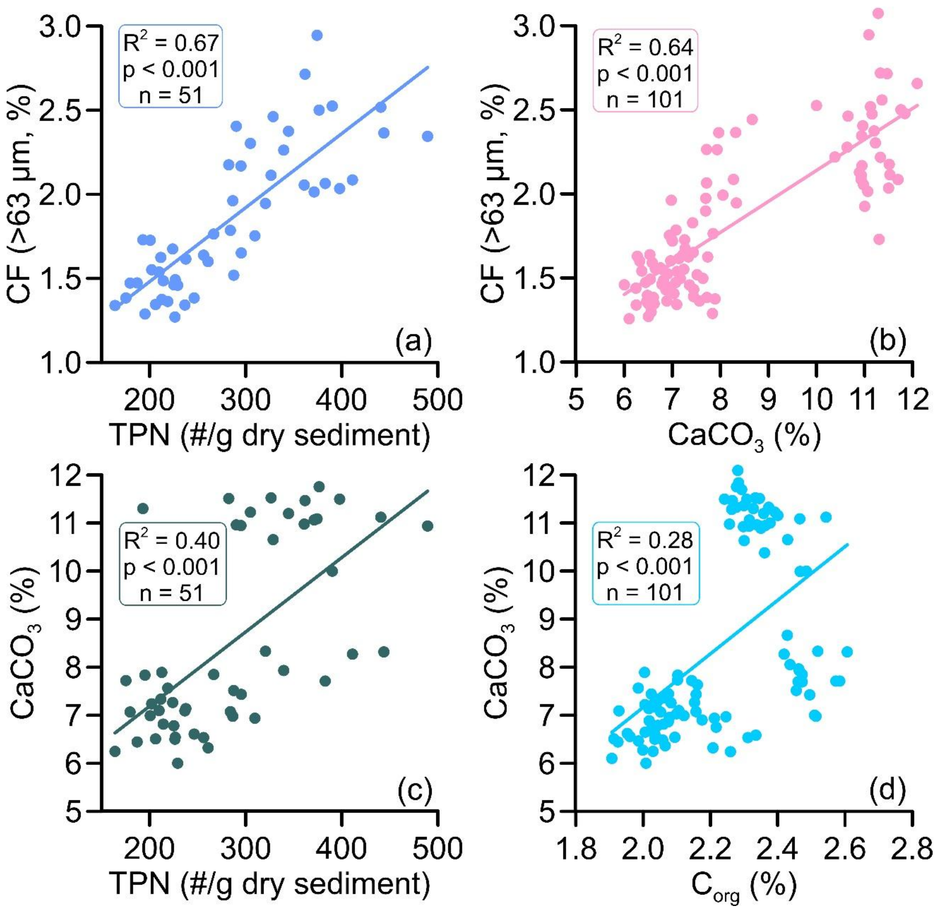


**Figure 5**

https://doi.org/10.5194/egusphere-2026-4747
Preprint. Discussion started: 1 September 2026


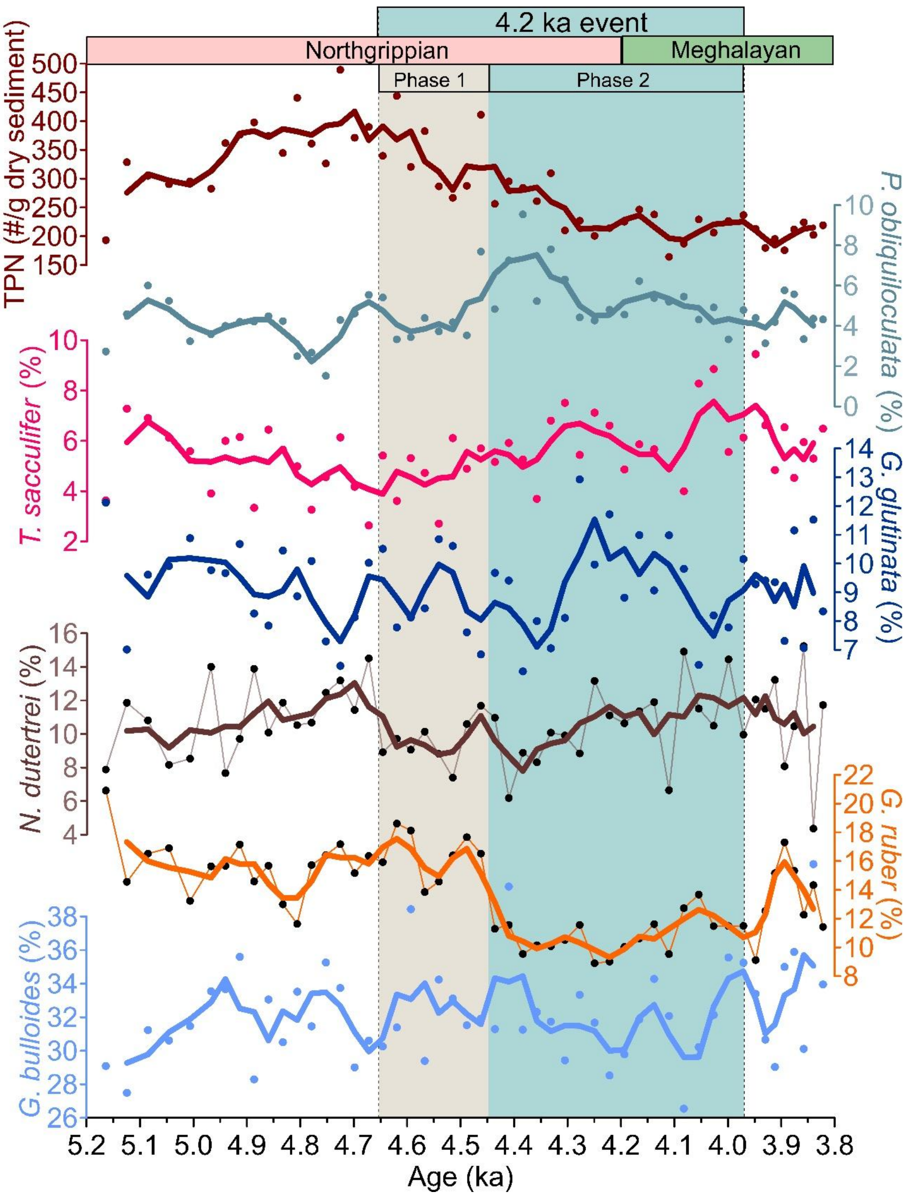


**Figure 6**

https://doi.org/10.5194/egusphere-2026-4747
Preprint. Discussion started: 1 September 2026




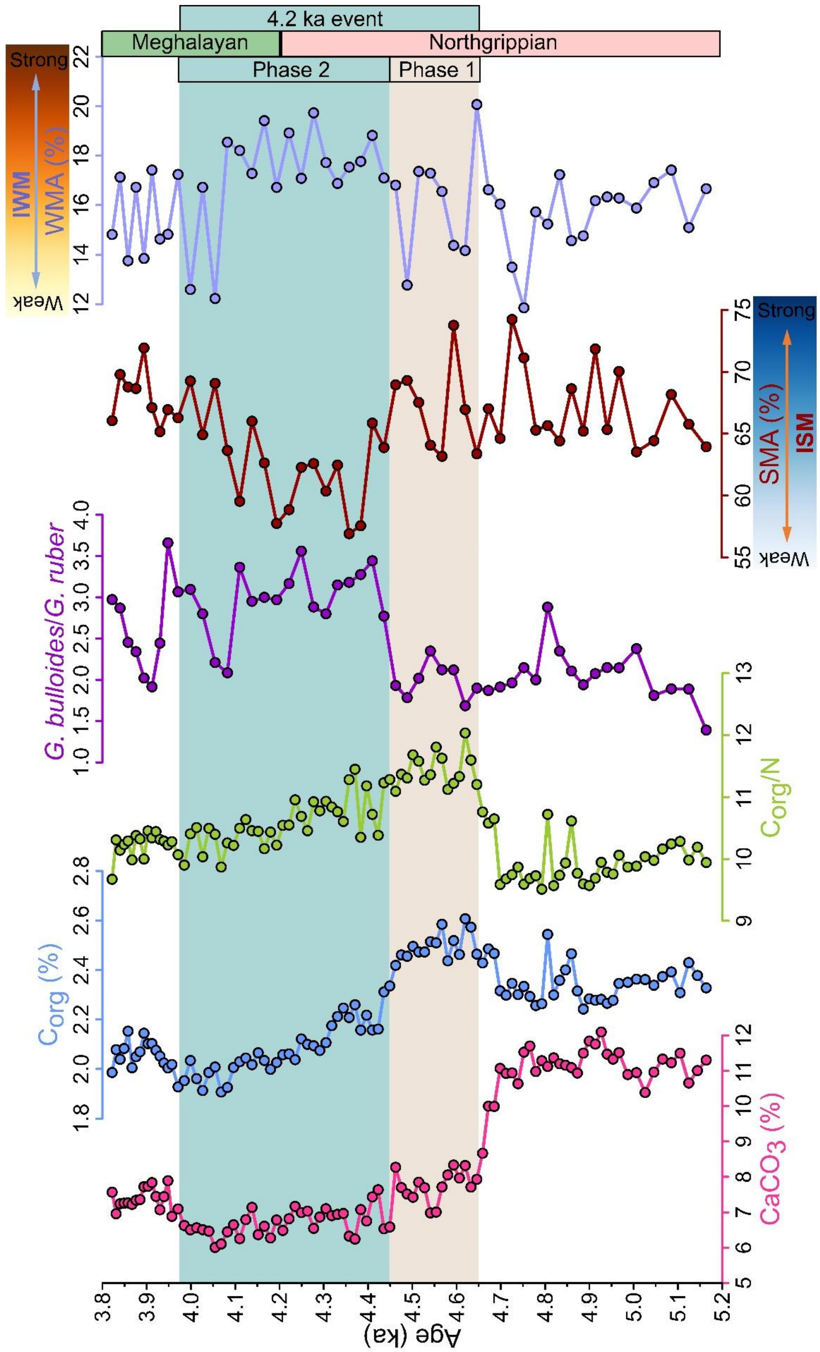


**Figure 7**

https://doi.org/10.5194/egusphere-2026-4747
Preprint. Discussion started: 1 September 2026


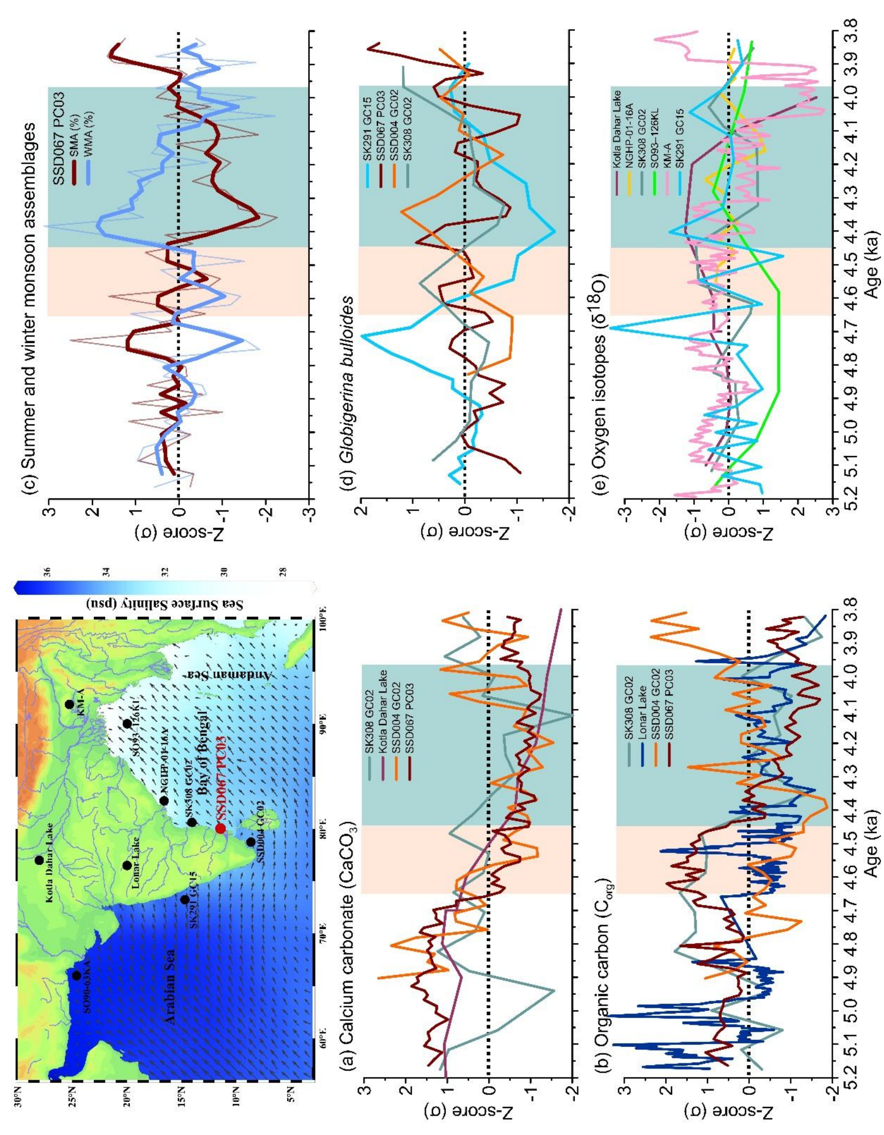


Figure 8

https://doi.org/10.5194/egusphere-2026-4747
Preprint. Discussion started: 1 September 2026




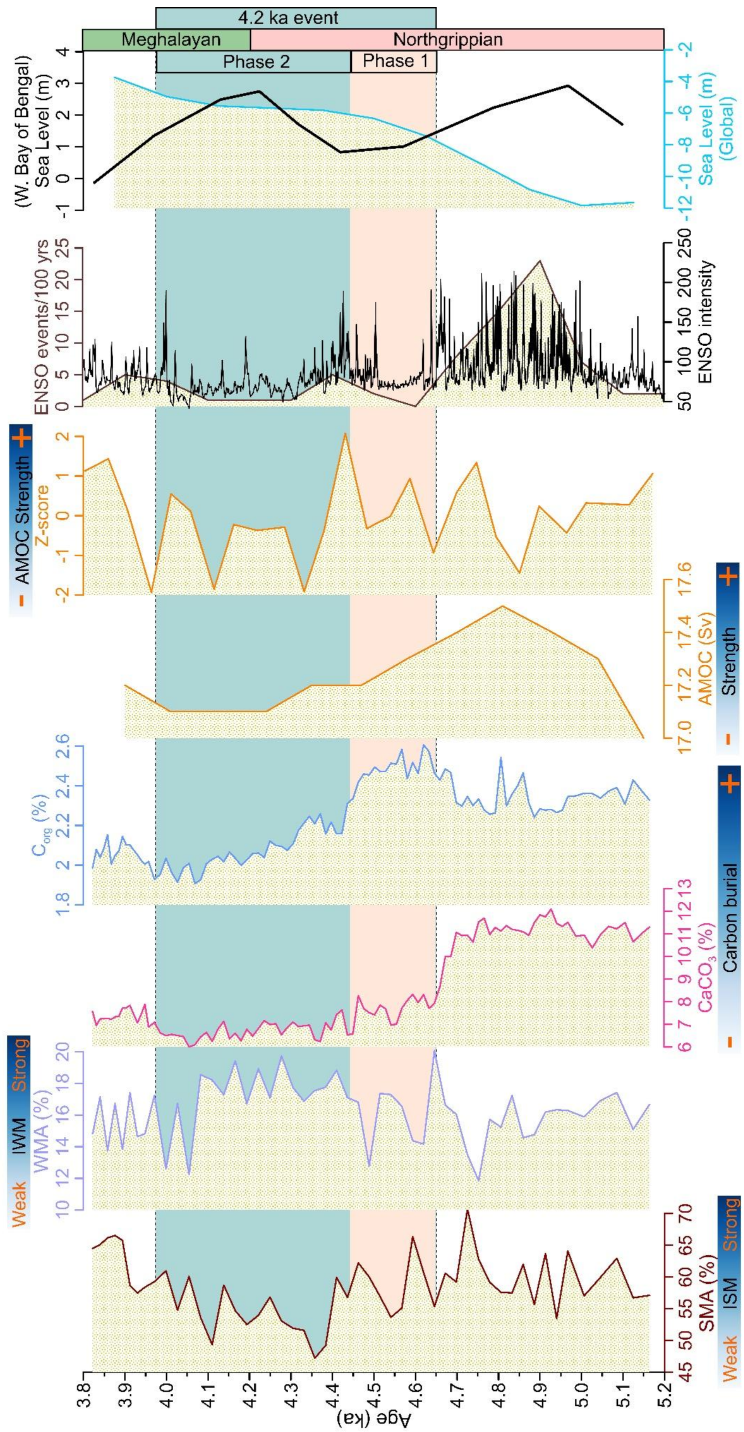


**Figure 9**

https://doi.org/10.5194/egusphere-2026-4747
Preprint. Discussion started: 1 September 2026


**Table 1**

| Sample Interval | Lab code | Radiocarbon Age (yr BP) | Error (± yr) | Cal. Age Range (2 sigma) (yr BP) | Cal. Median Age (ka) | Sedimentation Rate (cm/kyr) |
|---|---|---|---|---|---|---|
| 349-350 | IUACD#22C5197 | 3819 | 29 | 3556 - 3900 | 3.732 | 77.40 |
| 374-375 | IUACD#25C8619 | 3990 | 30 | 3790 - 4140 | 3.957 | 111.11 |
| 399-400 | IUACD#22C5198 | 4251 | 30 | 4128 - 4492 | 4.305 | 71.84 |
| 428-429 | IUACD#25C8620 | 4543 | 30 | 4509 - 4839 | 4.685 | 76.32 |
| 449-450 | IUACD#22C5199 | 4772 | 36 | 4808 - 5200 | 4.967 | 74.47 |
| 475-476 | IUACD#25C8621 | 5198 | 30 | 5308 - 5611 | 5.479 | 50.78 |
| 499-500 | IUACD#22C5200 | 5433 | 32 | 5578 - 5889 | 5.726 | 97.17 |

https://doi.org/10.5194/egusphere-2026-4747
Preprint. Discussion started: 1 September 2026


**Table 2**

| Proxy | Pre Event Mean | Event Mean | | Post Event Mean |
|---|---|---|---|---|
| | | Phase 1 | Phase 2 | |
| **Coarse Fraction (CF %)** | 2.41 | 1.97 | 1.49 | 1.49 |
| **Total Carbon (TC %)** | 3.67 | 3.41 | 2.88 | 2.95 |
| **Organic Carbon ($C_{org}$ %)** | 2.35 | 2.49 | 2.07 | 2.06 |
| **Total Inorganic Carbon (TIC %)** | 1.33 | 0.92 | 0.81 | 0.89 |
| **Nitrogen (N %)** | 0.24 | 0.22 | 0.20 | 0.20 |
| **Calcium Carbonate ($CaCO_3$ %)** | 11.07 | 7.69 | 6.71 | 7.39 |
| **$C_{org}$/N** | 9.96 | 11.43 | 10.56 | 10.23 |
| **Planktic Foraminifera (#/g dry sediment)** | 349 | 342 | 234 | 203 |
| ***Globigerina bulloides* (%)** | 31.66 | 32.53 | 32.06 | 33.64 |
| ***Globigerinoides ruber* (%)** | 15.67 | 16.46 | 10.85 | 13.44 |
| ***Neogloboquadrina dutertrei* (%)** | 11.02 | 9.54 | 10.52 | 10.83 |
| ***Globigerinita glutinata* (%)** | 9.24 | 8.85 | 9.19 | 9.18 |
| ***Trilobatus sacculifer* (%)** | 5.10 | 4.81 | 5.98 | 6.21 |
| ***Pulleniatina obliquiloculata* (%)** | 3.98 | 4.46 | 5.48 | 4.39 |
| ***G. bulloides/G. ruber*** | 2.05 | 1.99 | 2.99 | 2.59 |
| **Summer Monsoon Assemblage (%)** | 67.01 | 67.13 | 62.77 | 68.05 |
| **Winter Monsoon Assemblage (%)** | 15.67 | 16.17 | 17.25 | 15.39 |